Hole Solutions in the 1d Complex Ginzburg-Landau Equation

Stefan Popp[1], Olaf Stiller[1], Igor Aranson[2] and Lorenz Kramer[1]
[1] *Physikalisches Institut der Universität Bayreuth, D-95440 Bayreuth, Germany*
[2] *Department of Physics, Bar-Ilan University, Ramat Gan 52900, Israel*
(February 9, 2008)

The cubic Complex Ginzburg-Landau Equation (CGLE) has a one parameter family of traveling localized source solutions. These so called 'Nozaki-Bekki holes' are (dynamically) stable in some parameter range, but always structually unstable: A perturbation of the equation in general leads to a (positive or negative) monotonic acceleration or an oscillation of the holes. This confirms that the cubic CGLE has an inner symmetry. As a consequence small perturbations change some of the qualitative dynamics of the cubic CGLE and enhance or suppress spatio-temporal intermittency in some parameter range. An analytic stability analysis of holes in the cubic CGLE and a semianalytical treatment of the acceleration instability in the perturbed equation is performed by using matching and perturbation methods. Furthermore we treat the asymptotic hole–shock interaction. The results, which can be obtained fully analytically in the nonlinear Schroedinger limit, are also used for the quantitative description of modulated solutions made up of periodic arrangements of traveling holes and shocks.

PACS numbers: 47.20.-k; 05.45.+b

(Submitted to Physica D)

I. INTRODUCTION

Spatially extended oscillatory media in the weakly nonlinear regime can be described by a complex Ginzburg Landau equation (CGLE) which may be derived from an amplitude and slow-variation expansion [1]. In 1d it reads

$$\partial_t A = \left[1 + (1 + ib)\partial_x^2 - (1 + ic)|A|^2 + d|A|^4\right] A \tag{1}$$

where b and c are real constants . Length, time and the complex order parameter A have been scaled in the usual way for the cubic CGLE. In eq.(1) we have included a quintic term with a small complex prefactor $d = d' + id''$ ($|d| \ll 1$). We will refer to eq.(1) with $d \neq 0$ as the "perturbed (cubic) CGLE" and treat the d term only perturbatively to lowest order $O(d)$.

As already pointed out in reference [2] arbitrarily small $|d|$ may change the situation drastically, and eq.(1) without fifth order term ($d \equiv 0$) is not sufficient to describe the qualitative dynamics of the system in the parameter regime considered here, i.e. where Nozaki-Bekki hole solutions (see below) influence the dynamics. From the derivation of the CGLE one expects in a real physical system $d \propto \epsilon$ where ϵ is the distance from threshold. There are other corrections to the cubic CGLE which should have the same order of magnitude but their "perturbative effect" is expected to be rather similar and we have chosen the d term in eq.(1) to represent "higher-order perturbations". While in reference [2] we presented a phenomenological theory for phenomena observed numerically, in this work we will determine the important quantities of the theory with the help of analytical or semi-analytical methods.

Equation (1) has the family of traveling-wave solutions

$$A = R_q e^{i(qx-\omega(q)t)} \qquad \text{with} \quad R_q = \sqrt{1 - q^2 + d'(1 - q^2)^2}\,, \quad 0 \leq q^2 \leq 1 \tag{2}$$

and the dispersion relation

$$\omega(q) = cR_q^2 + bq^2 - d''R_q^4\,. \tag{3}$$

(As mentioned above all formulas are valid only at order d^1.)

A. Localized Solutions

Other important solutions are localized objects A_v moving with constant velocity v connecting asymptotic plane-wave states. In the co–moving frame ($\zeta = x - vt$) the plane-wave dispersion relation reads $\Omega(q, v) = \omega(q) - vq$.

Dealing with such constantly moving solutions it is convenient to write the CGLE (1) in a co–moving frame rotating with constant frequency Ω

$$\begin{aligned}\partial_t A(\zeta,t) \;&=\; F_{v,\Omega}[A] \\ &:= \left(1 + i\Omega + (1+ib)\partial_\zeta^2 + v\partial_\zeta - (1+ic)|A|^2 + d|A|^4\right) A\end{aligned} \tag{4}$$

Clearly, in order to ensure phase conservation, it is necessary that in this co–moving frame the plane waves on both sides rotate with the same frequency, i.e. $\omega(q_i) - vq_i = \Omega$ for $i = 1, 2$. From this and eqs.(2) and (3) one can derive the relation:

$$v = \frac{\omega(q_2) - \omega(q_1)}{q_2 - q_1} = 2(b-c)k - 2(cd' - d'')(R_{q_1}^2 + R_{q_2}^2)k \tag{5}$$

$$\text{with} \qquad k = \frac{1}{2}(q_1 + q_2) \tag{6}$$

Note that in the cubic CGLE this yields $v = 2(b-c)k$ which is the mean of the group velocity $\partial_q\omega(q)$ of the asymptotic plane waves. One differentiates between sources and sinks (often called shocks) depending on whether the group velocity (and thus causality) points inward or outward in the co-moving frame. Thus sources should determine the behavior of the asymptotic states while shocks are passive and play only a minor role. So in the following we will focus mainly on the investigation of sources.

For a standing ($v = 0$) (antisymmetric) source solution eq.(5) is fulfilled trivially due to symmetry ($q_1 = -q_2$). For $v \neq 0$, however, eq.(5) is not trivial at all and, as pointed out by van Saarloos and Hohenberg [3], the problem to find such source solutions of eq.(1) is in general overdetermined. Using counting arguments they showed that from a systematic point of view only standing sources should exist. Nevertheless the cubic CGLE (eq.(1) with $d = 0$) has an analytic one-parameter family of sources with different velocities v, the "hole solutions" of Nozaki and Bekki [4] (NB holes). They can be written in the form

$$\begin{aligned} A_v^{NB} &:= Z_v \exp(i\chi_v - i\Omega t) \\ &= [\hat{B}\partial_\zeta\varphi_v(\kappa\zeta) + \hat{A}v] \times \exp[i\varphi_v(\kappa\zeta) + i\hat{k}v\zeta - i\Omega t] \\ \text{where} \qquad & \varphi_v(\kappa\zeta) = \hat{\kappa}^{-1}\ln\cosh(\kappa\zeta) \;. \end{aligned} \tag{7}$$

Symbols with a "hat" denote constants depending only on b and c, e.g. $\hat{k} = 1/(2(b-c))$. The frequency Ω and κ^2 are linear functions of v^2. With exception of $\hat{A}$ all coefficients are real. The asymptotic plane waves for $\zeta \to \pm\infty$ have wavenumbers

$$q_{1/2} = k \pm K \qquad \text{with } \; K = \kappa/\hat{\kappa} \;, \quad k = v\hat{k} \;. \tag{8}$$

κ^2 becomes zero at a maximal velocity $\pm v_{max}$, and here the hole solution merges with a plane wave with wavenumber $q_1 = q_2 = v_{max}/(2(b-c))$. The relations are completely derived in Appendix A. The resulting algebraic equations (8 equations for 8 parameters) yield the one parameter family. The derivation in Appendix A demonstrates the necessary dependence in a transparent way.

The NB holes are connected with the 3-parameter family of dark soliton solutions that exist in the limit $b = \pm\infty,\ c = \pm\infty$, where eq.(1) reduces to the defocussing nonlinear Schroedinger equation (see next paper), and with the one-parameter family of static (all velocities collapse to zero) saddle-point solutions of the nonlinear diffusion equation obtained in the limit $b = c = 0$ [6]. Then one has a potential and the continuous family can be associated with (global) gauge invariance through Noether's theorem. Clearly then perturbations of the equation that preserve gauge invariance and the potential property, like a quintic term with a real prefactor, do not destroy the family.

An important result of this article is that in general the family of hole solutions is destroyed by the higher-order perturbation ($d \neq 0$) leaving only the standing hole. Thus moving NB holes are structurally unstable.

B. Stability and Destruction of Hole Solutions

The stability of the hole solutions (for $d = 0$) has first been investigated by Sakaguchi [7] in direct simulations of the CGLE. The perturbational equation of the CGLE (4) with $A = A_v + \mathcal{W}$ describing the stability problem

$$\partial_t\mathcal{W} = \mathcal{L}_v\mathcal{W} \qquad \text{with} \quad \mathcal{L}_v\mathcal{W} := \frac{\delta F_{v,\Omega}}{\delta A}[A_v]\,\mathcal{W} \;+\; \frac{\delta F_{v,\Omega}}{\delta A^*}[A_v]\mathcal{W}^* \tag{9}$$

(where now $A_v = A_v^{NB}$ and $\Omega = \Omega(v)$) describing the stability problem was then studied by Chaté and Manneville numerically for $v = 0, v = 0.2$ [8] and by Sasa and Iwamoto semianalytically for $v = 0$ [9]. As a result hole solutions were found to be stable in a narrow region of the b-c plane which is shown in Fig.1 for the standing hole ($v = 0$) . From below the region is bounded by the border of (absolute) stability of the emitted plane waves with wavenumber $q(b, c)$ (see eq.(7)) corresponding to the continuous spectrum of $\mathcal{L}_v$. From the other sides the stable range is bounded by the instability of the core with respect to localized eigenmodes corresponding to a discrete spectrum of $\mathcal{L}_v$. The core instability turns out to be connected with a stationary bifurcation where the destabilizing mode at threshold passes through the neutral mode $\mathcal{W} = \Phi_{tr}$ (see eq.(14)) of $\mathcal{L}_v$ which can be derived from translational invariance of the CGLE [8,9]. The cores of moving holes were found to be more stable than those of the standing ones [8].

Now we turn to the situation with small but finite d. Our simulations show that in the stable range moving holes are then in general either accelerated and eventually destroyed or slowed down and stopped to the standing hole solution depending on the phase of d. In particular for real $d = d'$ one has

$$\left[\frac{\partial_t v}{v}\right] \gtrless 0 \Leftrightarrow d' \gtrless 0 \tag{10}$$

One finds that the Nozaki-Bekki hole relations connecting the core velocity and the emitted wavenumbers (see eq.(7) and App.A) are (almost) satisfied at each instant during the acceleration process. The acceleration thus occurs approximately along the NB hole family and it can be described by taking $v = v(t)$ as a slowly varying variable while other degrees of freedom follow adiabatically.

From these numerical observations we conclude that for arbitrarily fixed values of b,c and varying d the standing hole solution undergoes a symmetry-breaking stationary bifurcation at $d = 0$. The (real) growth rate λ_d of the unstable mode is proportional to the acceleration

$$\lambda_d = \lim_{v \to 0} \dot{v}/v \ . \tag{11}$$

We will refer to this instability as the "acceleration instability" while the term "core instability" will be used for the bifurcation where b and/or c is changed while d is kept constant (including the case $d = 0$).

Of special interest is the case where the core-stability line is crossed with $d \neq 0$ (which actually corresponds to the physically relevant situation). Then the two modes which cause the acceleration instability and the (stationary) core instability (with $d \equiv 0$) are coupled which leads to a Hopf bifurcation. (nur bei d stabilisierend) As we showed in [2] the normal form for this bifurcation – valid for small d, v, u – is

$$\begin{aligned} \dot{u} &= (\lambda - sv^2)u + d_1 v \\ \dot{v} &= \mu u + d_2 v \ . \end{aligned} \tag{12}$$

Here u and v are the amplitudes of the core-instability and acceleration-instability modes respectively. s and μ are of order d^0 while $d_{1,2}$ must be of order d^1 since in the absence of a perturbation holes with nonzero velocity exist. For $d = 0$ the parameter λ can be identified with the growth rate of the core-instability mode. (In the general case λ has a correction proportional to d causing a shift of the threshold.) The nonlinear term in eq.(12) takes care of the fact that moving holes are more stable than standing ones and at the same time saturates the instability ($s > 0$).

Far away from the core-instability threshold where λ is strongly negative u can be eliminated adiabatically from eqs.(12) which yields

$$\dot{v} = (d_2 - d_1 \frac{\mu}{\lambda})v \tag{13}$$

The term in brackets can be identified as λ_d from eq.(11).

After introducing our general tools and concepts in Sec.II we will present a detailed perturbation analysis in Sec.III. Since the core instability (for the case $d = 0$) as well as the acceleration instability are of the stationary type (real growth rate) we will first investigate the stationary bifurcation scenario more closely in Sec.III A. Our approach allows to treat both instabilities within the framework of the same formalism. Then we will derive a fully analytic expression for the core instability line in the unperturbed equation ($d = 0$) (Sec.III B), present a semi-analytic method for treating the acceleration instability in the case $d \neq 0$ (Sec.III C) and investigate the interaction between holes and shocks in Sec.III D. A comparison of our analysis with simulations of the CGLE is presented in Sec.IV. Finally we will use our results for a quantitative description of moving periodically modulated solutions of the perturbed CGLE (Sec.V).

II. TOOLS AND CONCEPTS

A. The Linear Operator

The linear operator $\mathcal{L}_v$ introduced in eq.(9) has two bounded neutral modes

$$\mathit{\Phi}_{rot} = iA_v \qquad \mathit{\Phi}_{tr} = \partial_\zeta A_v \tag{14}$$

related to gauge and translational invariance of the CGLE.

For many applications it is convenient to introduce a transformation $W = \mathcal{W}\exp(-i\vartheta_v)$ where ϑ_v is some real field (often the phase of A_v). Equation (9) then goes over into

$$\partial_t W = L_v W := \exp(-i\vartheta_v)\mathcal{L}_v\left(\exp(i\vartheta_v)W\right) \quad . \tag{15}$$

For the NB solutions ($d = 0$) we choose $\vartheta_v = \chi_v$ obtaining

$$\begin{aligned} L_v^{NB}W &= \left((1+i\Omega) + (1+ib)(\partial_\zeta + i\partial_\zeta\chi_v)^2 + v(\partial_\zeta + i\partial_\zeta\chi_v) - 2(1+ic)|A_v^{NB}|^2\right)W - (1+ic)|A_v^{NB}|^2 W^* \\ &= (1{+}ib)\partial_{\zeta\zeta}W \;+\; \left(2Ki(1{+}ib)\tanh(\kappa\zeta) + 2ki(1{+}ic)\right)\partial_\zeta W \\ &+ \Big((1{+}ic)(-K^2\hat{B}^2\tanh^2(\kappa\zeta) + 2kK\tanh(\kappa\zeta) - 2v^2\hat{A}^2) + (1{+}i\Omega + (1{+}ib)iK\kappa)/\cosh^2(\kappa\zeta) + ivk - k^2(1{+}ib)\Big)W \\ &- \Big((1{+}ic)(v\hat{A} + K\hat{B}\tanh(\kappa\zeta))^2\Big)W^* \quad . \end{aligned} \tag{16}$$

Stationary instabilities are described by the eigenvalue problem related to eq.(15)

$$L_v W = \lambda W \tag{17}$$

with real λ. The bounded neutral modes from eq.(14) are now

$$\Phi_{rot} = iZ_v \;=\; i(v\hat{A} + K\hat{B}\tanh(\kappa\zeta)) \tag{18}$$

$$\Phi_{tr} = \partial_\zeta Z_v + iZ_v\partial_\zeta\chi_v \;=\; K\hat{B}\kappa/\cosh^2(\kappa\zeta) \;+\; (k + K\tanh(\kappa\zeta))\;\Phi_{rot}\;. \tag{19}$$

The other two fundamental modes satisfying $L_v^{NB}\Phi = 0$ (irrespective of boundary conditions) can be expressed in terms of generalized hypergeometric functions.

Asymptotically ($|\kappa\zeta| \gg 1$) one has plane waves, the operator L_v becomes space independent and the four fundamental modes behave exponentially $\sim e^{p_i\zeta}$. The exponents p_i ($i = 1...4$) can be obtained from the characteristic polynomial. Two of the exponents can be extracted from the bounded neutral modes Φ_{rot} and Φ_{tr} They are

$$p_1 = 0 \quad \text{and} \quad p_2 = \mp 2\kappa \qquad \text{for } \zeta \to \pm\infty \tag{20}$$

The other - in general complex - exponents p_3 and p_4 are given in Appendix B. Their real part is always positive/negative for $\zeta \gtrless 0$ showing that the other two fundamental modes are exponentially growing in space.

B. Condition for the Existence of a Family

A necessary condition for a standing hole solution $A_0 := A_{v=0}$ of the CGLE to be embedded in a continuous one-parameter family of moving hole solutions A_v can be obtained by taking the derivative of the stationary CGLE $F_{v,\Omega}[A_v] = 0$ with respect to v at $v = 0$:

$$\mathcal{L}_0\mathit{\Phi}_{fam}\left[= \left(\frac{\partial F_{v,\Omega}}{\partial v}\right)_{v=0}[A_0] = \partial_\zeta A_0\right] \;= \mathit{\Phi}_{tr} \qquad \text{with} \quad \mathit{\Phi}_{fam} = -\left.\frac{dA_v}{dv}\right|_{v=0} \tag{21}$$

(Here the fact has been used that for symmetry reasons Ω can only depend on v^2.) Equation (21) shows that the existence of a hole family implies that the translation mode $\mathit{\Phi}_{tr} = \partial_\zeta A_0$ has an inverse image $\mathit{\Phi}_{fam}$ under $\mathcal{L}_0 := \mathcal{L}_{v=0}$ which for large $|\zeta|$ grows linearly in space ($\mathit{\Phi}_{fam} \sim i\zeta A_v$) corresponding to an asymptotic wavenumber change (c.f.

eq.(22)). In the cubic case ($d = 0$) eq.(21) with this boundary condition is solved by inserting the Nozaki–Bekki solution $A_v = A_v^{NB}$. Then instead of eq.(21) one may write (c.f. eqs.(15,7,8))

$$L_0^{NB}\Phi_{fam} = \Phi_{tr} \ , \quad \text{with} \ \ -\Phi_{fam} \ = \ \hat{A} + i\hat{k}\hat{B}K\zeta\tanh(\kappa\zeta) \ . \tag{22}$$

In general ($d \neq 0$) all solutions of eq.(21) are found to diverge exponentially for $\zeta \to \pm\infty$ (see below) which is consistent with the fact that the hole family is destroyed by the higher-order perturbation. In the limit $0 \neq \left|\frac{b-c}{1+bc}\right| \ll 1$, which includes the relaxative case $b = c = 0$ as well as the conservative and fully integrable nonlinear Schroedinger limit ($b, c \to \infty$), we show this analytically in [5].

C. Motion within the Family – Asymptotic Matching

Above we stated that the acceleration of holes in the perturbed CGLE can be (approximately) described as a motion within the family of Nozaki-Bekki hole solutions by taking the family parameter $v = v(t)$ as slow variable. This would, however, lead to a change of the asymptotic wavenumbers (one has $\dot{k} = \hat{k}\dot{v}$) which is not possible in an infinite system. (As pointed out before the family mode $\Phi_{fam} = \partial_v A_v(\zeta, t)$, eqs.(21,22), describing the difference between two "neighboring" holes diverges linearly for large $|\zeta|$.) The difficulty is resolved by limiting the "motion within the family" to a finite region of size $\sim \dot{v}^{-1}$ around the hole core (inner region). A global solution for A has then to be constructed by asymptotic matching. For calculating the acceleration, however, it will not be necessary to perform the matching explicitly.

To illustrate this we consider the eigenvalue equation (17) with the condition

$$|W| < \ \text{bounded} \quad \text{for} \quad \zeta \to \pm\infty \tag{23}$$

describing the acceleration of the hole in the limit of small velocities (see next section). In the outer region

$$|\kappa\zeta| \gg 1 \qquad \text{(outer region)} \tag{24}$$

W behaves exponentially with exponents $p_i = p_i(\lambda)$ (c.f. Sec.II A, App.B). For values $0 < \lambda \ll 1$ there are two decaying ($p_{1/2}$) and two growing ($p_{3/4}$) exponents so that boundary condition (23) is indeed equivalent to

$$\text{'}W \text{ should not grow in space exponentially (with the exponents } p_{3,4})\text{'} \ . \tag{25}$$

It is crucial to note that because of the overlap of regions the realization of this boundary condition can already be controlled in the inner region without performing any matching.

Since there is one weakly decaying exponent $p_1 \sim \lambda \sim \dot{v}$ boundary condition (25) in practice leads to an algebraic growth of W (at the outer limit of the inner region). This can be understood as a truncated expansion of the exponentially decaying outer solution (see eq.(B8)) in the overlap region $W \sim (i + O(\lambda)) \left(1 + p_1\zeta + O(\lambda^2)\right)$. The portion $\sim ip_1\zeta$ corresponds to the linear divergence of Φ_{fam}. From this one finds the outer limit of the inner region

$$|p_1\zeta| \ll 1 \qquad \text{(inner region)} \ . \tag{26}$$

Boundary condition (25) is not restricted to the case of small velocities. Applied to the inner region it remains also valid in more realistic situations with slowly varying wavenumbers governed by phase equations far away from the hole core. We note that besides perturbations of the equation also core instability or modified boundary conditions (coming i.e. from the presence of a shock) in general lead to a hole acceleration which can be treated by an analogous matching approach.

III. PERTURBATION ANALYSIS

A. Formal Analysis of Stationary Instabilities

In this section we will investigate stationary instabilities of the standing hole with respect to localized modes. The formalism will be applicable to the acceleration instability in the perturbed CGLE and to the core instability in the cubic CGLE ($d = 0$).

Let $\mathbf{u} = (b, c, d)$ denote a point in parameter space of the CGLE . We write $\mathbf{u} = \hat{\mathbf{u}} + \Delta\mathbf{u}$ where $\hat{\mathbf{u}}$ belongs to the stability threshold. In particular $\hat{\mathbf{u}}$ may lie on the core-instability line $(b_{crit}, c_{crit}, d = 0)$, then $\Delta\mathbf{u} = (\Delta b, \Delta c, 0)$ is of interest (core instability), or $\hat{\mathbf{u}}$ can be a point $(b, c, 0)$ where the standing hole is stable and then $\Delta\mathbf{u} = (0, 0, d)$ (acceleration instability). We want to construct the unstable localized mode $W(x; \mathbf{u} = \hat{\mathbf{u}} + \Delta\mathbf{u})$ near the threshold. It satisfies

$$L_0(\mathbf{u})W(\mathbf{u}) = \lambda(\mathbf{u})W(\mathbf{u}) \tag{27}$$

where L_0 has been introduced in eqs.(9,15).

In the following we want to expand $W(\hat{\mathbf{u}} + \Delta\mathbf{u})$ in powers of $\Delta\mathbf{u}$. The calculations will be limited to the inner region (eq.26) where one may use boundary condition (25) instead of the usual condition (23) for localized modes. We will use the symbol Δu to denote the distance from threshold along a fixed path which crosses the neutral curve. Consistently the derivative $\frac{\partial}{\partial u}$ signifies the derivative along this path. At the threshold, $\lambda(\hat{\mathbf{u}}) = 0$, we have

$$W(\hat{\mathbf{u}}) = \Phi_{tr}(\hat{\mathbf{u}}) \ . \tag{28}$$

To see this we note that, since $W(\hat{\mathbf{u}})$ belongs to the null space of $L_0(\hat{\mathbf{u}})$, it has to coincide with one of the two neutral modes given in eq.(14). For reasons of symmetry one expects to have Φ_{tr}, which destroys the zero at the hole core.

Inserting the expansion

$$W(\hat{\mathbf{u}} + \Delta\mathbf{u}) = \Phi_{tr}(\hat{\mathbf{u}} + \Delta\mathbf{u}) + \Delta u W_1(\hat{\mathbf{u}}) + \Delta u^2 W_2(\hat{\mathbf{u}}) + O(\Delta u^3) \tag{29}$$

into eq.(27) one finds at first order in Δu

$$L_0(\hat{\mathbf{u}})W_1(\hat{\mathbf{u}}) = \frac{\partial\lambda(\hat{\mathbf{u}})}{\partial u}\ \Phi_{tr}(\hat{\mathbf{u}}) \ . \tag{30}$$

Equation (30) is proportional to eq.(21) and thus has the solution

$$W_1 = \frac{\partial\lambda(\mathbf{u})}{\partial u}\Big|_{\mathbf{u}=\hat{\mathbf{u}}} \Phi_{fam}(\hat{\mathbf{u}}) \ . \tag{31}$$

At second order in Δu eq.(27) then yields:

$$L_0(\hat{\mathbf{u}})\left(W_2(\hat{\mathbf{u}}) - \frac{1}{2}\frac{\partial^2\lambda(\hat{\mathbf{u}})}{\partial u^2}\ \Phi_{fam}(\hat{\mathbf{u}})\right) = \frac{\partial\lambda(\hat{\mathbf{u}})}{\partial u}\left(\frac{\partial\lambda(\hat{\mathbf{u}})}{\partial u}\Phi_{fam}(\hat{\mathbf{u}}) + \left[\frac{\partial\Phi_{tr}(\hat{\mathbf{u}})}{\partial u} - \frac{\partial L_0(\hat{\mathbf{u}})}{\partial u}\Phi_{fam}(\hat{\mathbf{u}})\right]\right) \tag{32}$$

where the term $\frac{1}{2}\frac{\partial^2\lambda(\hat{\mathbf{u}})}{\partial u^2}\Phi_{tr}(\hat{\mathbf{u}})$ was brought to the lhs with the help of eqs.(30) and (31). If a function $\Phi_{fam}(\hat{\mathbf{u}} + \Delta\mathbf{u})$ with

$$L_0(\hat{\mathbf{u}} + \Delta\mathbf{u})\Phi_{fam}(\hat{\mathbf{u}} + \Delta\mathbf{u}) = \Phi_{tr}(\hat{\mathbf{u}} + \Delta\mathbf{u}) \ . \tag{33}$$

exists at $\hat{\mathbf{u}} + \Delta\mathbf{u}$ the term in square brackets can be absorbed by modifying W_2. To see this one may expand W in the following way

$$W(\hat{\mathbf{u}} + \Delta\mathbf{u}) = \Phi_{tr}(\hat{\mathbf{u}} + \Delta\mathbf{u}) + \Delta u\frac{\partial\lambda(\hat{\mathbf{u}})}{\partial u}\Phi_{fam}(\hat{\mathbf{u}} + \Delta\mathbf{u}) + \Delta u^2\tilde{W}_2(\hat{\mathbf{u}}) + O(\Delta u^3) \tag{34}$$

which yields at second order in Δu :

$$L_0(\hat{\mathbf{u}})\left(\tilde{W}_2(\hat{\mathbf{u}}) - \frac{1}{2}\frac{\partial^2\lambda(\hat{\mathbf{u}})}{\partial u^2}\ \Phi_{fam}(\hat{\mathbf{u}})\right) = \left(\frac{\partial\lambda(\hat{\mathbf{u}})}{\partial u}\right)^2 \Phi_{fam}(\hat{\mathbf{u}}) \tag{35}$$

Equation (33), which is the condition for the existence of a hole family at $\hat{\mathbf{u}} + \Delta\mathbf{u}$, is satisfied near the core-instability line if d is kept zero. Thus the solvability of eq.(35) gives a criterion for the threshold of the core instability ($d = 0$) which will be evaluated fully analytically in the next section. Near the threshold of the acceleration instability however eq.(32) can only be fulfilled if

$$\frac{\partial\lambda(\hat{\mathbf{u}})}{\partial u} = \frac{\partial}{\partial d}\left[\frac{\dot{v}}{v}\right]_{d=0} \tag{36}$$

is adjusted properly which can be used to determine the acceleration of the holes. Thus the quantitative results for the acceleration of the holes given below represent a proof for the destruction of the hole family by the higher-order perturbation.

From eq.(32) one also sees that $\dot{v}/v$ diverges as one approaches the core-instability line in the b-c plane. Near this line however the analysis of this chapter looses its validity. Here the two modes leading to core and acceleration instability interact and the scenario becomes more complex (see eq.(12)).

B. Core Instability

In this section we calculate the core instability line in the cubic CGLE. We do this by giving a solvability condition for eq.(35) which we write in the form

$$L(\hat{\mathbf{u}})W(\hat{\mathbf{u}}) = \Phi_{fam}(\hat{\mathbf{u}}) \; . \tag{37}$$

Here Φ_{fam} is the family mode from eq.(22) and $L(\hat{\mathbf{u}}) = L_0^{NB}(b,c)$ is the linear operator around a standing hole (see eq.(16)). Equation (37) reads explicitly

$$\begin{aligned}(1+ib)\,\partial_{\zeta\zeta}W \;+\; (2iK(1+ib)\tanh(\kappa\zeta))\,\partial_\zeta W \;+\; (1+i\Omega+(1+ib)iK\kappa)\frac{1}{\cosh^2(\kappa\zeta)}\,W \;-\\ -\;(1+ic)(1-K^2)\tanh^2(\kappa\zeta)\,(W+W^*) \;\;=\;\; -K-2\kappa i \;+\; i(1-K^2)\zeta\tanh(\kappa\zeta)\end{aligned} \tag{38}$$

Solvability here means that we have to adjust the parameters $b = b(c)$ in a way that the (symmetric) solution W of this equation satisfies boundary condition (25). In a first step we simplify eq.(38) by making the following ansatz for W ("variation of constants")

$$\begin{aligned} W &= f_{rot}\Phi_{rot} + f_{tr}\Phi_{tr} \\ \text{where} \qquad \Phi_{rot} &= i\tanh(\kappa\zeta), \qquad \Phi_{tr} = 1/\cosh^2(\kappa\zeta) \;+\; (i/\hat{\kappa})\,\tanh^2(\kappa\zeta)\end{aligned} \tag{39}$$

are the two neutral modes of L_0 (c.f. eqs.(18,19)). f_{rot} and f_{tr} are two real functions to be determined. Inserting this ansatz into eq.(38) one gets after elimination of f_{rot} the following real second-order differential equation for $f := \partial_\zeta f_{tr}$

$$\begin{aligned} \hat{L}f &= I_{fam} \\ \text{where} \quad \hat{L} \;&:=\; \partial_{\zeta\zeta} - 6\kappa\tanh(\kappa\zeta)\partial_\zeta + \big((6K^2+12\kappa^2)\tanh^2(\kappa\zeta) - 4\kappa^2\big) \\ I_{fam} \;&:=\; 6K^2\zeta\cosh^2(\kappa\zeta) + 3K^2(b\hat{\kappa}-2)\zeta + (b+bK^2-4K^2\hat{\kappa})3K/(1-K^2)\;\tanh(\kappa\zeta)\cosh^2(\kappa\zeta)\end{aligned} \tag{40}$$

From the asymptotic behavior ($|\zeta| \to \infty$) of eq.(40) one easily sees that the only boundary condition for the (anti-symmetric) function $f = \partial_\zeta(\cosh^2(\kappa\zeta)Re(W))$ which is compatible with condition (25) for W is given by

$$f \sim \zeta e^{2\kappa|\zeta|} \quad \text{for } \zeta \to \pm\infty \; . \tag{41}$$

This excludes the behavior $\sim e^{(2\kappa + p_{3/4})|\zeta|}$ of the two fundamental modes of $\hat{L}$. Equations (40,41) can be solved with the ansatz

$$f = \sum_{m=-1}^{\infty} c_m\zeta\cosh^{-2m}(\kappa\zeta) \;+\; \sum_{m=-1}^{\infty} d_m\tanh(\kappa\zeta)\cosh^{-2m}(\kappa\zeta) \tag{42}$$

As shown in Appendix C for certain values of (b,c) with $b = b(c)$ one can adjust the coefficients $c_m,\ d_m$ in a way that the series converges uniformly towards a smooth function solving the boundary value problem eqs.(40,41). The condition for convergence defines the core instability line. Explicitly this line is given by

$$\tfrac{1-K^2}{1+\hat{\kappa}^2}\,S(\hat{\kappa}^2) \;+\; 1 \;+\; K^2\,\tfrac{3b-14\hat{\kappa}}{3b+2\hat{\kappa}} \;=\; 0 \tag{43}$$

$$\begin{aligned} \text{where} \quad S(\hat{\kappa}^2) &:= \frac{3}{4+3/\hat{\kappa}^2} \;+\; \sum_{n=2}^{\infty}\frac{2n+1}{2n^2+2n+3/\hat{\kappa}^2}\,\prod_{m=2}^{n}\frac{2m^2-m+3/\hat{\kappa}^2}{2m^2+m+3/\hat{\kappa}^2} \\ &= \frac{3}{4+3/\hat{\kappa}^2} \;+\; \frac{\Gamma(\frac{9}{4}+a)\Gamma(\frac{9}{4}-a)}{\Gamma(\frac{7}{4}+a)\Gamma(\frac{7}{4}-a)}\,\sum_{n=2}^{\infty}\frac{2n+1}{2n^2+2n+3/\hat{\kappa}^2}\,\frac{\Gamma(n+\frac{3}{4}+a)\Gamma(n+\frac{3}{4}-a)}{\Gamma(n+\frac{5}{4}+a)\Gamma(n+\frac{5}{4}-a)} \\ &\text{with} \;\; a := \frac{1}{4}\sqrt{1-24/\hat{\kappa}^2}\end{aligned} \tag{44}$$

In the limit of large c one can neglect the first term in eq.(43) which contains the infinite sum $S(\hat{\kappa}^2)$ and eq.(43) reduces to

$$\text{either} \qquad b^4 = \frac{16}{9}c^2 + O(c^{3/2}) \quad \text{for } c \to \infty \quad (b > 0) \tag{45}$$

$$\text{or} \qquad b = -1/\sqrt{2} + O(1/c) \quad \text{for } c \to \infty \tag{46}$$

Eqs.(45) describe both branches of the core instability line in the limit $c \to \infty$. The core instability line (43) together with the curve describing the instability of the plane waves at the wings of the hole give the complete stability diagram of the standing Nozaki-Bekki hole solution. The curves are plotted in Fig.1. They are consistent with previous results [7] [8] [9] and generalize them. Finally we remind that our derivation made use of the fact that the core instability occurs via a static bifurcation, which was first found by [8] and [9].

C. Acceleration Instability

In the following we treat the acceleration of a moving hole caused by a perturbation of the cubic CGLE. We use adiabatic elimination which in the limit $v \to 0$ can be put into the framework introduced in section III A. We assume that in the perturbed CGLE the hole acceleration occurs near the hole family and can be described by taking $v = v(t)$ as the slow variable while the other degrees of freedom follow adiabatically. Formally this is done by writing

$$A = (Z_{v(t)}(\zeta) + W(\zeta)) \ \exp\left(i\chi_{v(t)}(\zeta) - i\int_0^t \left(\Omega_{v(\tau)} + \Delta\Omega\right) d\tau\right); \qquad \zeta := x - \int_0^t v(\tau)d\tau \tag{47}$$

where Z_v, χ_v, Ω_v describe the slowly time dependent NB hole. $W, \Delta\Omega$ are the small changes of the solution caused by the quintic perturbation. At lowest order they are time independent (adiabatic elimination). As before this ansatz is only valid in the inner region (26). Inserting (47) into the CGLE (4) in the co-moving frame rotating with frequency $\Omega_{v(t)} + \Delta\Omega$ one obtains

$$\dot{v}\partial_v A = F_{v(t)\ \Omega_{v(t)}+\Delta\Omega}[A] \tag{48}$$

The only time dependence which cannot be transformed away by this choice of the coordinate system is given by a movement within the family $\dot{v}\partial_v A$. $W, \dot{v}, \Delta\Omega$ are of order d. Using the fact that A_v^{NB} solves the cubic CGLE $F^{d=0}_{v\ \Omega}[A_v^{NB}] = 0$ at each time t and neglecting all higher order terms in d one arrives at the following ordinary linear differential equation for the perturbation W

$$\begin{aligned} L_v^{NB} W \ &= \ I_v(\Delta\Omega, \dot{v}) \\ \text{where} \qquad I_v(\Delta\Omega, \dot{v}) &:= \dot{v}\Phi_{fam} - i\Delta\Omega Z_v - d|Z_v|^4 Z_v \end{aligned} \tag{49}$$

Here one has to adjust the parameters $\Delta\Omega, \dot{v}$ in the inhomogeneity in such a way that the solution W satisfies (25) which determines the acceleration $\dot{v}$.

Equations (32) and (49) can both serve to calculate the acceleration sufficiently far away from the core instability line (where it is possible to replace eq.(12) by eq.(13)). While eq.(49) is applicable for holes moving with arbitrary velocities v (but small $\dot{v}$) eq.(32) is only valid for small v. The connection between both equations can be seen by expanding (49) in terms of v. Writing

$$\begin{aligned} L_v^{NB} &= L_v^{NB(0)} + vL_v^{NB(1)} + O(v^2) \\ W &= W^{(1)} + vW^{(2)} + O(v^2) \\ I_v &= I^{(1)} + vI^{(2)} + O(v^2) \end{aligned} \tag{50}$$

and remembering that $L_v^{NB(0)} = L_0^{NB}$ is the linear operator from eq.(38) describing perturbations around the standing hole of the cubic CGLE, eq.(49) becomes at order v^0

$$\begin{aligned} L_0^{NB} W^{(1)} &= I^{(1)} \\ &= -i\Delta\Omega Z_0 - dZ_0^5 \end{aligned} \tag{51}$$

Here $I^{(1)}$ and thus $W^{(1)}$ are antisymmetric. $W^{(1)}$ has to satisfy the boundary condition (25) which fixes the parameter $\Delta\Omega$. $W^{(1)}$ and $\Delta\Omega$ describe the changes of a standing hole resulting from a d–perturbation in the cubic CGLE. These changes have already been included in the approach of subsection III A. $W^{(1)}$ and $\Delta\Omega$ can be found analytically (see eq.(D13)). At order v^1 eq.(49) then reads

$$L_0^{NB} W^{(2)} = -L_v^{NB(1)} W^{(1)} + I^{(2)}$$
$$= -L_v^{NB(1)} W^{(1)} + \frac{\dot v}{v}\Phi_{fam} - i\Delta\Omega \hat{A} - dZ_0^4(3\hat{A} + 2\hat{A}^*) \qquad (52)$$

This equation corresponds to eq.(32). The r.h.s., and thereby the perturbation $W^{(2)}$, are symmetric and one has to adjust the acceleration $\frac{\dot v}{v}$ such that $W^{(2)}$ fulfills the boundary condition (25). (Note that in deriving eq.(52) we have expanded the equation of motion (48) in d and afterwards in v whereas eq.(32) can be found from eq.(48) by an interchange of the expansions.) For small d, v one has

$$\frac{\dot v}{v} = Re(g^* d) + O(v^2) \qquad g := g_1 + ig_2 \qquad (g_i \text{ real}) \qquad (53)$$

In Section IV A eq.(49) will be used to determine g numerically for arbitrary b, c while in App.D eq.(52) will be used to calculate g analytically in the NLS-limit ($b, c \to \infty$).

D. Hole – Shock Interaction

The acceleration of a hole as calculated in the last subsection is influenced in the presence of a shock. Here we treat this acceleration in the limit of large hole–shock separation. For that purpose we divide space into overlapping hole and shock regions. The important point is that when using the ansatz (47) in the hole region the boundary condition (25) is changed by the shock. In the region of overlap one now has (besides decaying $\sim e^{p_{1/2}\zeta}$) growing stationary perturbations $\sim e^{p_{3/4}\zeta}$ forming the shock out of the plane-wave state. The distance from the shock determines the magnitude of the growing perturbation (prefactor of W) and thus the hole acceleration.

The hole–shock interaction depends crucially on the fact whether the growing exponents $p_{3/4}$ are real or complex conjugated. Accordingly one has monotonic ('monotonic case') or oscillatory ('oscillatory case') interaction (see below eqs.(57,58)). The boundary between the two interaction types in the b, c–parameter plane is given by the condition $p_3 = p_4$ which depends on the hole velocity v since $p_{3/4} = p_{3/4}(v)$ (c.f.App.B). In particular for a standing hole the boundary line becomes

$$\hat\kappa^2 - 6 = 0 \qquad (54)$$

which is included in Fig.1 ($\hat\kappa$ is given in eq.(A8).).

In the overlap range ($\kappa^{-1} \ll \zeta \ll L$) between the hole position $\zeta = 0$ and the shock position $\zeta = L$ (defined by $\partial_\zeta arg(A)|_{\zeta=L} = 0$) one has approximately plane waves plus linear perturbations W of the form (c.f.App.B)

$$We^{-i\phi} = r_3 e^{p_3\zeta + i\phi_3} + r_4 e^{p_4\zeta + i\phi_4} \qquad \text{(monotonic case)} \qquad (55)$$
$$\text{or} \quad We^{-i\phi} = z e^{p_3\zeta} + \eta(p_3) z^* e^{p_3^*\zeta} \qquad \text{(oscillatory case).} \qquad (56)$$

(Here $\phi := arg(v\hat{A} + K\hat{B})$ is a fixed phase factor.) The perturbations are made up of the two growing fundamental modes of L_v. The two real prefactors $r_{3/4} = r_{3/4}(L)$ or the complex constant $z = z(L)$ describing the contribution of these modes have to be determined from the asymptotic shape of the shock solution (see below). They depend exponentially on the distance L between hole and shock with reversed exponents $\sim e^{-p_{3/4}L}$. Thus the L dependence of the acceleration induced by the perturbation W is given by

$$\dot v = g_3 e^{-p_3 L} + g_4 e^{-p_4 L} \qquad \text{(monotonic case)} \qquad (57)$$
$$\text{or} \quad \dot v = g_3 e^{-Re(p_3)L} \sin(Im(p_3)L + g_4) \qquad \text{(oscillatory case)} \quad . \qquad (58)$$

The two unknown real constants g_3, g_4 have to be determined from solving eq.(49) with boundary condition (57,58) instead of (25). In the monotonic case the smaller exponent p_4 ($p_3 > p_4 > 0$) dominates asymptotically and for practical purposes the coefficient g_4 is (usually) sufficient to describe the acceleration.

Now we turn to the calculation of the constants $r_{3/4}$ or z from the asymptotics of the shock solution. Besides the long–wavelength approximation, where after a Hopf Cole transformation the shock region is described by a linear phase equation (see [5]), there exists no analytic expression for the shock solution. Therefore in general the constants r_3, r_4, z have to be calculated numerically by solving a boundary value problem (c.f.Sec.IV A). In addition a crude analytic estimate can be obtained by the following 'linear approximation': we extend the hole region up to the center of the shock which means that the shock is a superposition of a plane wave and the linear perturbations $\sim e^{p_{3/4}\zeta}$.

Assuming $\partial_\zeta A|_{\zeta=L}=0$ at the position $\zeta=L$ of the shock (which corresponds to a standing shock) one gets by using again (47)

$$\begin{aligned} & \partial_\zeta \left((Z_{v(t)}+W)e^{i\chi_{v(t)}}\right)\Big|_{\zeta=L} = 0 \\ \overset{\kappa L \gg 1}{\Longleftrightarrow} \quad & \left(\partial_\zeta W + iq_1\left(v\hat{A}+K\hat{B}+W\right)\right)\Big|_{\zeta=L} = 0 \end{aligned} \tag{59}$$

Inserting W from eq.(55) or (56) one obtains an approximate expression for $r_{3/4}(L)$ or $z(L)$ respectively.

So far we have only treated the interaction of one hole and one shock in the cubic CGLE. In general boundary conditions (55,56) apply on both sides of the hole separately with corresponding shock distances $L_{(r/l)}$. In most cases, however, one of the hole–shock interactions dominates and the constants $r_{3/4}$ or z can be set zero on the other side (corresponding to the interaction with a shock infinitely far away). In any case the full information on the boundary condition for W can be gathered into one real four vector $\vec{b}$ containing the boundary constants r_3, r_4 or z for both sides. Since in the perturbed CGLE the hole acceleration depends linearly on this boundary vector $\vec{b}$ and on the d–perturbation (via the inhomogeneity of eqs.(49,52)) one may simply add the hole accelerations caused by neighboring shocks (eqs.(57,58)) and d–perturbations of the CGLE (eq.(53)). This is exploited in the next section.

IV. NUMERICAL RESULTS AND COMPARISON WITH SIMULATIONS

A. Numerical Methods

We now show how one can determine numerically the hole acceleration induced by a d-perturbation or an interaction with a shock. Mathematically this means solving the differential equation (49) with the boundary conditions (25) or (55,56) described by the boundary vector $\vec{b}$.

First let us assume the vector $\vec{b}$ were known. One has to adjust $\dot{v}, \Delta\Omega$ in eq.(49) in a way that the solution W is asymptotically described by $\vec{b}$. This can be achieved by the following 'shooting' method. One integrates eq.(49) (numerically) starting at $\zeta=0$. The correct initial values $W(0)$ and $\partial_\zeta W(0)$ are unknown but one may assume without loss of generality $Re(W(0))=0$ and $Im(\partial_\zeta W(0))=0$, which can always be achieved by a suitable addition of the neutral modes Φ_{rot} and Φ_{tr} to the perturbation W. One is left with two real parameters $Im(W(0))$ and $Re(\partial_\zeta W(0))$ describing the initial condition and two further real parameters $\dot{v}, \Delta\Omega$ occuring in the inhomogeneity of eq.(49). Now one integrates eq.(49) from $\zeta=0$ once to (sufficiently large) positive ζ and once to negative ζ with all four parameters set zero. From the asymptotic growth of W at the wings one can read off a real four vector $\vec{b}_0$ describing this growth. Doing similar integrations with the following values of the parameters one obtains the boundary vectors $\vec{b}_i,\ (i=1...4)$.

$$\begin{array}{lllll} Im(W(0))=1 & Re(\partial_\zeta W(0))=0 & \dot{v}=0 & \Delta\Omega=0 & \Rightarrow \quad \vec{b}_1 \\ Im(W(0))=0 & Re(\partial_\zeta W(0))=1 & \dot{v}=0 & \Delta\Omega=0 & \Rightarrow \quad \vec{b}_2 \\ Im(W(0))=0 & Re(\partial_\zeta W(0))=0 & \dot{v}=1 & \Delta\Omega=0 & \Rightarrow \quad \vec{b}_3 \\ Im(W(0))=0 & Re(\partial_\zeta W(0))=0 & \dot{v}=0 & \Delta\Omega=1 & \Rightarrow \quad \vec{b}_4 \end{array} \tag{60}$$

Because of the linearity of the boundary value problem one can now determine the set of parameters corresponding to the desired boundary vector $\vec{b}$. Solving the linear equation

$$\vec{b}_0 + Im(W(0))(\vec{b}_1-\vec{b}_0) + Re(\partial_\zeta W(0))(\vec{b}_2-\vec{b}_0) + \dot{v}(\vec{b}_3-\vec{b}_0) + \Delta\Omega(\vec{b}_4-\vec{b}_0) = \vec{b} \tag{61}$$

yields the acceleration $\dot{v}$ and the frequency shift $\Delta\Omega$, which the hole receives under the influence of neighboring shocks and/or a d-perturbation. One needs two of these runs for the calculation of g_1, g_2 (eq.(53)) and two further runs for the calculation of g_3, g_4 (eqs.(57,58)).

Now we turn to the determination of the constants r_3, r_4, z in eqs.(55,56). Since the shock solution connects two plane–wave states it is described by the ODE (4) $F^{d=0}_{v_s\Omega_s}[A]=0$ with the shock velocity v_s and frequency Ω_s fixed by the (given) wavenumbers q_1, q_2 at the wings. We solved this boundary value problem using a NAG routine. In some intermediate region between the system boundaries and the center of the shock the amplitude is just given by the incoming plane waves and linear perturbations $\sim e^{p_{3/4}\zeta}$ growing towards the shock center. In this region we extract the desired constants r_3, r_4, z.

Our simulations of the CGLE (1) were performed with a pseudospectral code based on FFT using a predictor corrector scheme in time. We had to use very high precision in the simulations, because discretization errors, like

the d-perturbation, in general destroy the inner symmetry of the cubic CGLE and therefore have similar effects on the hole solution, i.e. they also lead to an acceleration. Typically we used discretizations of $\Delta x \sim 0.05 - 0.15$ and $\Delta t \sim 0.001 - 0.02$ depending on the parameters b, c, d of the CGLE.

B. Results

Next we compare the results from the semianalytical calculations in sections III C,III D with those of direct simulations of the CGLE.

Figure 2 shows the acceleration of a hole center caused by a quintic perturbation of the CGLE. The acceleration formula (53) with the constant g obtained from the numerical matching (using eqs.(49,25)) is seen to be in good agreement with the simulations. This also confirms that the acceleration instability is indeed of stationary type. When scanning the (b, c)–range of stable hole solutions one always finds deceleration for (real) $d < 0$, consistent with the simulations. From the fully analytical treatment in App.D (c.f. eq.(D14)) it is seen that this result remains valid in the nonlinear Schroedinger limit. (Then one has numerical problems with the matching because here the ratio $|p_3/p_4|$ of the two growing exponents p_3, p_4 tends to infinity which prevents a correct numerical extraction of the boundary vectors b_i (c.f. section IV A).)

As already stated in section III D the (b, c, d)–region of stable hole solutions is divided into parts with monotonic and with oscillatory interaction between holes and shocks. Figures 3a,3b show the acceleration of a standing hole under the influence of a standing shock solution for both interaction types in the case $d = 0$. Here in the direct simulations the shock solutions were simply modeled by taking $\partial_\zeta A = 0$ at the system boundaries. As a result one has almost perfect quantitative agreement of simulations and numerical matching if in the latter the shock is treated nonlinearly, i.e. when the parameters r_3, r_4 (or z) in the boundary conditions (55,56) are extracted from a numerical solution of the shock boundary value problem. With the 'linear approximation' (59) one obtains only qualitative agreement. When scanning the monotonic interaction range with the matching routine we found that the asymptotic hole shock interaction is always attractive. Near the nonlinear Schroedinger limit one has monotonic interaction (see Fig.1). Here one can calculate analytically the hole-shock interaction (see [5]) and it also turns out to be always attractive.

V. ARRANGEMENTS OF HOLES AND SHOCKS

In this section we use the results from the previous sections for the description of stable states made up of a periodic arrangements of holes and shocks. Such states are frequently observed in simulations with periodic boundary conditions (see e.g. [11], [2]). Figure 4 shows the modulus $|A| = |A(x)|$ of a typical solution found in a simulation. As shown in Fig.5 one finds uniform as well as (almost) harmonic and strongly anharmonic oscillating hole velocities. (Slightly) beyond the core instability line the direction of the velocity is changed in the oscillations (see Fig.5d). The solutions are seen to be very sensitive to d–perturbations of the cubic CGLE.

The uniformly moving solutions can be well understood from the results of the last sections. First one has to note that they are not expected to be stable (and we indeed could not observe them in simulations) in the monotonic range [1] since here the asymptotic hole–shock interaction is always attractive (c.f. section IV B). Therefore we may restrict ourselves to the case of oscillatory interaction. Away from the core instability line uniformly moving periodically modulated solutions can then be identified as fixed points of a first order differential equation for the hole velocity v as the only slow variable. The other degrees of freedom are thereby assumed to follow adiabatically.

One equation for the hole velocity v is obtained by considering the acceleration caused by interaction with a neighboring shock at distance L together with that resulting from a d–perturbation. From eqs.(53,58) one obtains in the limit of small velocities v

$$\dot{v} \ = \ v \ Re(g^* d) \ + \ g_3 e^{-p_3'(v)L} \sin(p_3''(v)L + g_4) \ , \qquad g = g_1 + i g_2 \ , \qquad p_3 = p_3' + i p_3'' \tag{62}$$

Here we have taken into account only the interaction of the hole with one of the neighboring shocks, implicitly assuming that the period P of the solution satisfies $P \gg L$ in addition to $\kappa L \gg 1$, which is necessary for the

[1] The boundary between monotonic and oscillatory interaction depends on the hole velocity (see III D).

asymptotic analysis. Equation (62) is correct up to first order in v if the two matching parameters $g_{3,4}$ are calculated including corrections linear in v and $\dot{L}$ in the matching procedure (i.e. $g_3(v,\dot{L}) = g_{30} + vg_{3v} + \dot{L}g_{3\dot{L}}$). In the following we eliminate the two unknowns $L, \dot{L}$.

The shock velocity $v_s = v + \dot{L}$ is determined by the incoming (plane) waves via a generalization of eq.(5) to slowly varying solutions leading to

$$v_s = v + O(\dot{v}) \; . \tag{63}$$

Thus $\dot{L} = O(\dot{v})$ can be neglected in the matching parameters g_3, g_4 occurring in eq.(62) (since the factor $e^{-p_3'(v)L}$ is small).

From periodicity one has the condition that the phase along one period P of the solution is an integral multiple of 2π. Using the fact that the full phase ϕ of a NB–hole solution is given by

$$\begin{aligned} \phi(\zeta) &= \chi_v(\zeta) + arg(Z_v(\zeta)) \\ &\approx K|\zeta| - \ln 2 + k\zeta + arg(v\hat{A} \pm K\hat{B}) \qquad \text{for } \pm\kappa\zeta \gg 1 \end{aligned} \tag{64}$$

one can derive the phase condition

$$2\pi n \;\stackrel{!}{=}\; \phi(P) - \phi(0) \;\approx\; 2KL + P(k-K) + arg\left(\frac{v\hat{A} + K\hat{B}}{v\hat{A} - K\hat{B}}\right) \;+\; \phi_s(v) \qquad (n \in \mathbf{N}) \tag{65}$$

Here ϕ_s is the phase change due to the presence of the shock. For symmetry reasons $\phi_s = \phi_s(q_1, q_2)$ with $q_i = q_i(v)$ is an antisymmetric function of the hole velocity v and it becomes linear for small velocities. Solving (65) for L and linearizing in v one gets

$$L \approx L_{nP} - g_5 v \qquad \text{with: } L_{nP} := \frac{1}{2}\left(P + (2n-1)\pi/K\right), \quad g_5 := \frac{1}{2K}\left(\left.\frac{\partial\phi_s}{\partial v}\right|_{v=0} + \frac{k}{v}\left(P + \frac{2\hat{A}''}{K\hat{B}}\right)\right) \tag{66}$$

Inserting eqs.(63) and (66) into eq.(62) one arrives at a differential equation for v of the desired form

$$\dot{v} = f_{nP}(v) \tag{67}$$

describing solutions with n, P as parameters in addition to b, c, d. In the derivation we have assumed stationary (or at most slowly evolving) solutions as well as small velocities. Furthermore we have neglected d–corrections in the plane wave quantities $(k, K, p_{3,4}, ...)$. All parameters $(g_1, .., g_5)$ can be extracted from the matching procedure and the numerical nonlinear shock solution.

The implications of eq.(67) are very simple. The fixed points ($\dot{v} = 0$) describe the uniformly traveling states. Their velocity $v_{fp} = v_{fp}(n, P)$ and hole–shock separation $L_{fp} = L_{fp}(n, P)$ are predicted by eq.(67) as functions of n, P. Their stability (within the family parameter v) is determined by the sign of the linear growth rate $\lambda_{fp} := \partial f_{nP}/\partial v|_{v_{fp}}$. In Figs.6,7 these theoretical predictions for $v_{fp}(n, P)$ and $L_{fp}(n, P)$ are compared with data from numerical simulations for the CGLE parameters $b = 0.5,\ c = 2.3,\ d = \pm 0.0025$. The full lines describe stable solutions ($\lambda_{fp} < 0$) while dashed lines correspond to unstable ones ($\lambda_{fp} > 0$). The theoretical results are seen to be well confirmed by the numerical simulations especially in the limit of small velocities. The remaining discrepancies can be explained by the neglect of the d-corrections in the plane wave quantities $(k, K, p_{3,4}, ...)$ and the linearization in v. Note that for fixed period P several stable solutions can coexist which may (but don't have to) differ by the phase $2\pi n$ contained in one period (see Fig.6).

The essential influence of the d–perturbation on the solutions is especially apparent for very slowly solutions (c.f. eq.(62))

$$v_{fp} \approx -(1/Re(g^* d))\; g_{30}\; e^{-p_3'(0)L_{nP}}\; \sin(p_3''(0)L_{nP} + g_{40}) \tag{68}$$

occuring in the limit of small interaction $e^{-p_3' L_{nP}} \ll |d| \ll 1$. Since one then has $\lambda_{fp} \approx Re(g^* d)$ these solutions are only stable for decelerating d–perturbation. As a consequence for accelerating d (slowly) uniformly moving solutions exist stably only for certain periods (see Fig.7) whereas in the opposite case such solutions occur for arbitrary values of P (see Fig.6). This fact is well confirmed in our simulations.

Now we turn to the solutions with oscillating hole velocities. In our simulations we found such solutions coexisting (stably) with uniformly moving solutions but they occurred especially for parameters where eq.(67) does not have

stable fixed points (see Figs.5b,5c). The solutions are characterized by the occurrence of large velocities ($v \sim 1$) and interaction strengths ($e^{p_3'(v)L} \sim 1$) during the oscillations. Presumably they can (in a first approximation) be identified as stable limit cycles of a two dimensional dynamical system with the hole velocity v and the hole–shock distance L as active variables. While one has $\dot{L} = O(\dot{v})$ (as in eq.(63)) $\dot{v}$, and thus $\dot{L}$, cannot be neglected now. Thus from the phase conservation condition one obtains an evolution equation for $\dot{L}$ which has to be combined with the equation for the hole acceleration $\dot{v}$ yielding the two dimensional dynamical system. In this description eqs.(66,67) correspond to the adiabatic elimination of $\dot{L}$.

The mechanism for the oscillations beyond the core stability boundary (see Fig.5d) is of different nature. Here the core instability mode introduces a new degree of freedom. While for accelerating d this leads to a destruction of the solutions, in the decelerating case the interplay of core and acceleration instability leads to a Hopf bifurcation of the fixed point solutions of eq.(67) similar to the situation described for isolated holes by eq.(12). This yields the oscillating solutions of Fig.5d.

VI. CONCLUDING REMARKS

The investigation presented in this paper is of general importance since the CGLE is generally derived from an amplitude expansion near the threshold of a bifurcation and higher-order perturbations appear naturally. Of course there should be other terms of the same magnitude as the quintic term included in eq.(1). However, since the effects described above are closely related to phase conservation one should expect the other terms to have the same qualitative consequences and it should be possible to describe a physical system with a single "effective" higher-order term. We expect the consequences of our results to be restricted to (quasi-)1-dimensional systems in the vicinity of the parameter range where hole solutions are stable in the (unperturbed) cubic CGLE. Thus stable, uniformly moving holes should in general not be observable. (Note that in the case where the background state carries traveling waves rather than homogeneous oscillations, the CGLE (1) has an additional group velocity term. Motion then has to be defined with respect to a frame moving with that group velocity.)

The detailed investigation of spatio-temporal chaos presented by Shraiman et al. [12] for the unperturbed CGLE is presumably robust with respect to perturbations because the sensitive parameter range is not considered there. A later investigation [11] considers the sensitive range, where the determination of the range of existence of spatio-temporal chaos becomes questionable in the unperturbed CGLE. We found that stable hole solutions suppress spatio-temporal chaos and as a consequence for a stabilizing perturbation the (upper) boundary of spatio-temporal chaos is simply given by the stability boundary HS (see Fig.1) of the NB hole solutions, whereas for destabilizing perturbation spatio-temporal chaos is also observed further up [2].

Comparing holes in 1d with spirals in 2d one can state that spirals behave in a rough sense (apart from topological stability) similar to holes in the perturbed CGLE with stabilizing (decelerating) perturbation. Thus one has a range (which is in 2d very large) where standing spirals are core stable. For large values of $|b|$ a core instability occurs, which is of Hopf type [13]. In contrast to the 1d case the bifurcation is subcritical in 2d and leads to spatio-temporal chaos. We also note that the theory of interaction between localized solutions is similar in 1d and 2d [14].

Transient hole-type solutions were observed experimentally by Lega et al. [15] in the (secondary) oscillatory instability in Rayleigh-Bénard convection in an annular geometry. Here one is in a parameter range where holes are unstable in the cubic CGLE, so that small perturbations are irrelevant. Long time stable stationary holes ('1d spirals') were observed in a quasi-1d chemical reaction system (CIMA reaction) undergoing a Hopf bifurcation by Perraud et al. [16]. The experiments were performed in the vicinity of the cross-over (codimension-2 point) from the (spatially homogeneous) Hopf bifurcation to the spatially periodic, stationary Turing instability. Simulations of a reaction-diffusion system (Brusselator) with appropriately chosen parameters exhibited the hole solutions (and in addition more complicated localized solutions with the Turing pattern appearing in the core region). It seems likely that for the hole solutions the vicinity of the codimension-2 point is not important, and that the parameters correspond to the stable hole range in the CGLE description with stabilizing perturbations.

Finally we mention recent experiments by Leweke and Provencal [17] where the CGLE is used to describe results of open-flow experiments on the transitions in the wake of a bluff body in an annular geometry. Here the sensitive parameter range is reached and in the observed amplitude turbulent states holes should play an important role.

We wish to thank S.Sasa for sending us data of the core instability line in addition to those in [9]. One of us (I.A.) wishes to thank the Alexander-von-Humboldt Stiftung for financial support and the University of Bayreuth for its hospitality. Support by the Deutsche Forschungsgemeinschaft (Kr-690/4, Schwerpunkt 'Strukturbildung in dissipativen kontinuierlichen Systemen: Experiment und Theorie im quantitativen Vergleich') is gratefully acknowledged.

APPENDIX A: THE NOZAKI-BEKKI HOLE SOLUTIONS

Inserting the ansatz (7) into the CGLE one obtains a polynomial of third order in $\partial_\zeta \varphi_v(\kappa\zeta) \equiv K \tanh(\kappa\zeta)$ ($K := \kappa/\hat{\kappa}$). Requiring that terms at each order cancel separately one is confronted with 4 complex equation for 8 real parameters so that a priori one should only expect a discrete solution. The 4 complex equations, however, are not independent, which leads to the one parameter family of hole solutions. In the following we derive the explicit form of the Nozaki-Bekki hole solutions in a way which shows this dependence from the structure of the CGLE and the solutions. (Results are listed in eqs.(A8 – A12)). Introducing (7) into the CGLE one obtains

$$\left(L_{lin}[v,k,\Omega] - (1+ic)|Z_v|^2\right) Z_v e^{i\varphi_v} = 0 \quad , \qquad Z_v = \hat{B}\partial_\zeta \varphi_v(\kappa\zeta) + \hat{A}v \tag{A1}$$

with the linear operator $\quad L_{lin}[v,k,\Omega] := 1 - k^2 + i(\Omega + v^2\hat{k} - bk^2) + V\partial_\zeta + (1+ib)\partial_\zeta^2$

and $V := v(1+2i(1+ib)\hat{k} \equiv v\hat{V})$. Using the fact that L_{lin} commutes with the operator $(-i\hat{B}\partial_\zeta + v\hat{A})$ one easily finds

$$L_{lin} Z_v e^{i\varphi_v} = L_{lin}(-i\hat{B}\partial_\zeta + v\hat{A})e^{i\varphi_v} = \left[\Lambda Z_v - \hat{B}i\partial_\zeta\Lambda\right] e^{i\varphi_v} \tag{A2}$$

with the "eigenvalue" $\Lambda = \Lambda(\partial_\zeta\varphi_v) := \exp(-i\varphi_v) L_{lin} \exp(i\varphi_v) = z(\partial_\zeta\varphi_v)^2 - iV\partial_\zeta\varphi_v + 1 + i(\Omega + v^2\hat{k}) + i(1+ib)(\hat{\kappa}K^2 - k^2)$ and $z := (1+ib)(i\hat{\kappa} - 1)$. Introducing this into eq.(A1) one sees that $\partial_\zeta\Lambda/Z_v$ has to be a polynomial of second order in $\partial_\zeta\varphi_v = K\tanh(\kappa\zeta)$ and one finds

$$\Lambda = z\hat{B}^{-2}Z_v^2 + const. \tag{A3}$$

from which follows

$$i\hat{V} = 2z\hat{A}\hat{B}^{-1} \ . \tag{A4}$$

Using eqs.(A2) and (A3) equation (A1) reduces to

$$\Lambda - (1+ic)|Z_v|^2 = 2iz\hat{B}^{-1}\partial_\zeta Z_v \tag{A5}$$

which is of second order in $\partial_\zeta\varphi_v$. Dividing this equation by z the real part has the form:

$$\hat{B}^{-2} Re(Z_v^2) - Re(\frac{1+ic}{z})|Z_v|^2 = const. \tag{A6}$$

(where the fact that $\partial_\zeta Z_v = \hat{B}\partial_{\zeta\zeta}\varphi_v$ is real was used). Noting that $Re(Z_v^2) = (\partial_\zeta\varphi_v + v\hat{A}')^2 - \hat{A}''^2 = |Z_v|^2 + const$ one finds that the equations obtained from the nonconstant contributions – those proportional to $(\partial_\zeta\varphi_v)^1$ and $(\partial_\zeta\varphi_v)^2$ – are equivalent. In this way one can convince oneself that the remaining equations are indeed not independent.

To get the explicit solutions from eq.(A5) one may proceed as follows. At order $(\partial_\zeta\varphi_v)^2$ one obtains a complex equation

$$(1+ic)\hat{B}^2 = (1+2i\hat{\kappa})z \equiv (1+2i\hat{\kappa})(1+ib)(i\hat{\kappa}-1) \tag{A7}$$

which determines $\hat{B}$ and $\hat{\kappa}$:

$$\hat{\kappa} = \frac{1}{4(b-c)}\left(3(1+bc) + \sqrt{9(1+bc)^2 + 8(b-c)^2}\right) \tag{A8}$$

and

$$\hat{B} = \sqrt{\frac{3\hat{\kappa}(1+b^2)}{b-c}} \ . \tag{A9}$$

From order $\partial_\zeta\varphi_v^1$ contributions of eq.(A5) one gets another complex equation which together with eq.(A4) yields a set of 3 independent real equations for $\hat{k}, \hat{A}'$ and $\hat{A}''$. Solving them one obtains

$$\hat{A}' = -\hat{B}^{-1} \qquad \hat{A}'' = -2\frac{\hat{\kappa}}{\hat{B}} \qquad \text{and} \quad \hat{k} = [2(b-c)]^{-1} \tag{A10}$$

where the last formula is identical with the phase-conservation condition (5). From constant terms ($\sim (\partial_\zeta \varphi_v)^0$) one can derive the dispersion relation (in the moving frame)

$$\Omega = c - vk + (b-c)(k^2 + K^2) \tag{A11}$$

and an elliptic relation which relates the two not yet specified variables v and κ (or $K \equiv \kappa/\hat{\kappa}$) to each other:

$$v^2(\hat{k}^2 + |\hat{A}|^2) + K^2(1+\hat{B}^2) = 1 \; . \tag{A12}$$

Thus one finds indeed a one parameter family of moving hole solutions which can be labeled e.g. by their velocity. From eq.(A12) one finds that κ becomes zero at $v = v_{max} \equiv \left[\hat{k}^2 + |\hat{A}|^2\right]^{-1}$.

APPENDIX B: ASYMPTOTIC ANALYSIS OF NOZAKI–BEKKI HOLE SOLUTIONS

In the limit $\zeta \to \pm\infty$ the NB hole solutions (7) become plane waves with wavenumber $q_{1/2} := k \pm K$ (see eq.(8)) and frequency $\omega(q_{1/2}) = c + (b-c)q_{1/2}^2$ (see eq.(3)). The perturbational equation for these plane waves in a coordinate system moving with the velocity v of the hole core reads

$$\partial_t W = (1+ib)\,\partial_{\zeta\zeta} W \;+\; (v + 2iq_{1/2}(1+ib))\,\partial_\zeta W \;-\; (1+ic)(1-q_{1/2}^2)\,(W + W^*) \tag{B1}$$

This equation coincides with the asymptotic ($|\kappa\zeta| \gg 1$) perturbational equation (15) with L_v from eq.(16) (after transforming away an (irrelevant) fixed phase factor $W \to W e^{-iarg(v\hat{A} \pm K\hat{B})}$). Equation (B1) can be solved by an exponential ansatz

$$W = z e^{p\zeta + \lambda t} + z_* e^{p^*\zeta + \lambda^* t} \qquad\qquad \text{with} \quad p, \lambda, z, z_* \text{ complex} \tag{B2}$$

Inserting this into eq.(B1) yields two complex linear equations for the constants z, z_*^* whose solvability condition leads to characteristic equation

$$\begin{aligned} p^4(1+b^2) \;+\; p^3\, 2v \;+\; p^2 \left(4q_{1/2}^2 + (v - 2bq_{1/2})^2 - 2(1+bc)(1-q_{1/2}^2) - 2\lambda\right) \\ +\; p\, \left((4(b-c)q_{1/2} - 2v)(1-q_{1/2}^2) + (4bq_{1/2} - 2v)\lambda\right) \;+\; \left(\lambda^2 + 2\lambda(1-q_{1/2}^2)\right) \;=\; 0 \end{aligned} \tag{B3}$$

The four roots $p_i = p_i(v, \lambda)$ describe the possible asymptotic spatial behavior of perturbations W with growth rate λ in the coordinate system co-moving with the velocity v of the hole core. In particular the exponents $p_i = p_i(v)$ describing stationary perturbations are obtained for $\lambda = 0$. For $\zeta \to +\infty$ one finds

$$\begin{aligned} p_1 = 0, \qquad p_2 = -2\kappa \\ p_{3/4} = \kappa - \frac{v}{1+b^2} \;\pm\; \sqrt{-4q_1^2 - 3\kappa^2 + 2(1-q_1^2)\frac{1+bc}{1+b^2} + \frac{4bq_1 v + 2\kappa v - v^2}{1+b^2} + \frac{v^2}{(1+b^2)^2}} \end{aligned} \tag{B4}$$

For $v = 0$ one has $q_1 = -q_2$ and the expression for $p_{3/4}$ simplifies

$$p_{3/4} = \kappa \pm \sqrt{\kappa^2 - 6q_1^2} \tag{B5}$$

The exponents p_i for $\zeta \to -\infty$ can be found from eqs.(B4,B5) by the replacement $q_1 \to q_2$ and reversal of the overall signs. In the following we will for simplicity only treat the case $\zeta \to +\infty$. The exponents p_1 and p_2 describe the asymptotics of the two neutral modes eqs.(18,19). The exponents $p_{3/4}$ being real (monotonic case) or complex conjugated (oscillatory case) always satisfy

$$Re(p_{3/4}) > 0 \; , \tag{B6}$$

which shows that two fundamental modes of L_v^{NB} are exponentially growing in space. For each p_i the constants $z(p_i), z_*(p_i)$ can be found from the eigenvector equation. One finds

$$z_* = \eta z^*$$
$$\text{where} \quad \eta(p_i) := \left(\frac{p_i^2(1+ib) + p_i(v - 2bq_1 + 2iq_1)}{(1+ic)(1-q_1^2)} - 1 \right)^* \tag{B7}$$

For real p_i (which covers the exponents p_1, p_2 and in the monotonic case also p_3, p_4) one has $|\eta(p_i)| = 1$ and the asymptotic behavior of the stationary perturbation associated with one of the exponents p_i is given by

$$W \sim e^{p_i\zeta + i\phi_i} \quad \text{where } \phi_i := \frac{1}{2} arg(\eta(p_i)) \qquad \text{for } \zeta \to \infty \qquad (p_i \text{ real}) \tag{B8}$$

In the case $p_3 = p_4^*$ complex W behaves asymptotically like

$$W = ze^{p_3\zeta} + \eta(p_3)(ze^{p_3\zeta})^* \qquad \text{for } \zeta \to \infty \qquad (p_3 \text{ complex}) \tag{B9}$$

The complex quantity z gives the two growing fundamental modes in the perturbation W. We note that depending on the velocity v of the hole the behavior of the growing perturbations $\sim e^{p_{3/4}\zeta}$ may be quite different on both wings; in particular it may be oscillatory on one and monotonic on the other wing.

Now we turn to the situation of a small nonzero growth rate ($|\lambda| \ll 1$). Then the exponents from eq.(B4) are slightly changed. In particular the exponent $p_1 = p_1(v, \lambda)$ describing the outer asymptotics of localized modes bifurcating through the translation mode Φ_{tr} (e.g. the core instability mode) becomes near their bifurcation

$$p_1 \approx \frac{\lambda}{v - 2|q_1(b-c)|} \qquad \text{for} \quad |\lambda| \ll 1 \tag{B10}$$

Performing a similar analysis of asymptotic plane wave states in the perturbed CGLE ($0 \neq |d| \ll 1$) most of the foregoing expressions receive d–corrections. However, since translational (and rotational) invariance are preserved by the perturbed equation, the stationary ($\lambda = 0$) exponent $p_1 = 0$ remains unchanged and also eq.(B10) for small λ remains valid at lowest order in d. Therefore eq.(B10) describes (besides the core instability mode in the cubic CGLE) also the acceleration mode in the perturbed CGLE.

APPENDIX C: CORE INSTABILITY

In this section we present the solution of the boundary value problem eqs.(40,41) defining the core instability line utilizing the ansatz (42). From the relations

$$\hat{L}\,(\zeta \cosh^{-2n}(\kappa\zeta)) = \cosh^{-2n}(\kappa\zeta)\, \left(N_n\zeta - M_n^c\zeta\cosh^{-2}(\kappa\zeta) - R_n\tanh(\kappa\zeta)\right) \tag{C1}$$
$$\hat{L}\,(\tanh(\kappa\zeta)\cosh^{-2n}(\kappa\zeta)) = \cosh^{-2n}(\kappa\zeta)\, \left(N_n\tanh(\kappa\zeta) - M_n^d\tanh(\kappa\zeta)\cosh^{-2}(\kappa\zeta)\right) \tag{C2}$$
$$\text{with} \quad N_n := 4n^2\kappa^2 + 12n\kappa^2 + 8\kappa^2 + 6K^2, \quad R_n := 4\kappa n + 6\kappa \tag{C3}$$
$$M_n^c := 4n^2\kappa^2 + 14n\kappa^2 + 12\kappa^2 + 6K^2, \quad M_n^d := 4n^2\kappa^2 + 18n\kappa^2 + 20\kappa^2 + 6K^2, \tag{C4}$$

follows, that when inserting (42) into eq.(40), one can in a first step recursively determine the coefficients c_m and then in the next step the coefficients d_m from the c_m. In summary one has

$$c_{-1} = 1, \qquad c_0 = \frac{\Delta_1}{N_0}, \tag{C5}$$
$$c_m = \frac{\Delta_1}{N_m}\prod_{n=0}^{m-1}\frac{M_n^c}{N_n} \tag{C6}$$
$$d_{-1} = \frac{\Delta_2}{N_{-1}}, \tag{C7}$$
$$d_m = \frac{1}{N_m}\{d_{m-1}M_{m-1}^d + c_m R_m\} = \frac{1}{N_m}\,\left(\prod_{n=0}^{m}\frac{M_{n-1}^d}{N_{n-1}}\right)\left\{\Delta_2 + \Delta_1\frac{N_{-1}}{M_{-1}^d}\left(\frac{R_0}{N_0} + \sum_{n=1}^{m}\frac{R_n}{N_n}\prod_{k=0}^{n-1}\frac{M_k^c}{M_k^d}\right)\right\} \tag{C8}$$

where

$$\Delta_1 := 2\kappa^2 + 3b\kappa K, \qquad \Delta_2 := \tfrac{K}{1-K^2}(3b + 3bK^2 - 14\hat{\kappa}K^2 + 2\hat{\kappa}) \tag{C9}$$

From eq.(C6) follows that for large m the coefficients c_m behave like

$$c_m \;=\; \frac{\Delta_1}{N_m}\prod_{n=0}^{m-1}\frac{M_n^c}{N_n} \;\sim\; \frac{1}{m^2}\prod_{n=0}^{m-1}\frac{1+\frac{7}{2n}}{1+\frac{3}{n}} \;\sim\; m^{-3/2} \quad \text{for } m\to\infty \tag{C10}$$

Therefore the first sum in (42) always converges uniformly towards a smooth function. Because of

$$\frac{1}{N_m}\prod_{n=0}^{m-1}\frac{M_n^d}{N_n} \;\sim\; \frac{1}{m^2}\prod_{n=0}^{m-1}\frac{1+\frac{9}{2n}}{1+\frac{3}{n}} \;\sim\; m^{-1/2} \quad \text{for } m\to\infty \tag{C11}$$

the coefficients d_m in eq.(C8) may behave like $\sim m^{-3/2}$ or $\sim m^{-1/2}$ depending on whether the curly bracket in eq.(C8), which behaves like $const + O(1/m)$, gives zero in the limit $m\to\infty$ or not. In the latter case the second sum in the ansatz eq.(42) converges (pointwise) towards a function with a finite step at $\zeta = 0$ whereas in the first case the limiting function is smooth everywhere. Therefore one has to adjust (b, c) with $b = b(c)$ in a way that the curly bracket in eq.(C8) vanishes for $m\to\infty$. This determines the core instability line. Resubstitution of $N_m, M_m^c, ...$ into the curly bracket of eq.(C8) yields the final expression (43).

APPENDIX D: ACCELERATION INSTABILITY IN THE NONLINEAR SCHROEDINGER LIMIT

In this section we present a method to treat the acceleration instability in the NLS-limit ($b, c\to\infty$) by making use of the formalism introduced in subsections II C,III A,III C. We calculate the acceleration by projecting the (symmetric) inhomogeneity of eq.(52) onto the symmetric neutral mode Φ_s of the adjoint operator [2] $L^\dagger := L_0^{NB\,\dagger}$. The scalar product vanishes only for suitably adjusted parameter $\frac{\dot v}{v}$ in the inhomogeneity and this ensures the solvability of eqs.(52,25).

Using the scalar product

$$\langle U, W\rangle := \int_{-\infty}^{\infty} Re(U^* W)dx \tag{D1}$$

the adjoint problem is

$$L^\dagger\Phi_s = 0 \qquad \text{with} \qquad |\Phi_s|\to 0 \qquad \text{for } \zeta\to\pm\infty \tag{D2}$$

$$L^\dagger\Phi_s \;=\; (1-ib)\,\partial_{\zeta\zeta}\Phi_s \;+\; (2iK(1-ib)\tanh(\kappa\zeta))\,\partial_\zeta\Phi_s \;+\; (1-i\Omega+(1-ib)iK\kappa)\frac{1}{\cosh^2(\kappa\zeta)}\,\Phi_s \;- \\ -\,(1-ic)(1-K^2)\tanh^2(\kappa\zeta)\,\Phi_s -\; (1+ic)(1-K^2)\tanh^2(\kappa\zeta)\,\Phi_s^*$$

In analogy to Appendix B an investigation of the asymptotics of the fundamental modes of $L^\dagger$ shows that for $|\kappa\zeta|\gg 1$ they behave like $\sim e^{p_i|\zeta|}$. For $\zeta\to\infty$ the exponents p_i are

$$p_1 = 0, \qquad p_2 = +2\kappa, \qquad p_{3/4} = -\kappa \pm \sqrt{\kappa^2 - 6K^2} \tag{D3}$$

These are just the exponents of L with reversed sign (c.f. eqs.(B4,B5)). The two decaying exponents $p_{3/4}$ describe the desired symmetric mode Φ_s in the outer region ($|\kappa\zeta|\gg 1$) of the asymptotic matching procedure. In the NLS limit one finds with the help of the relations of App.A

$$p_{3/4} = -\kappa \pm \kappa\left(1 - \frac{4(b-c)^2}{3b^2c^2} + O(b^{-4})\right) \tag{D4}$$

Both exponents are real ('monotonic range') and $p_3\to 0$ for $b, c\to\infty$. The contribution to Φ_s proportional to $e^{p_3\zeta}$ has a prefactor z_3 with

---

[2] In this section we drop the indices '0' and 'NB' to simplify the notation.

$$\frac{Im(z_3)}{Re(z_3)} = -\left(\frac{1}{c} + O(b^{-3})\right) \tag{D5}$$

as can be calculated in analogy to (B8). The inner region is defined by $|p_3\zeta| \cong |\kappa\zeta\frac{4(b-c)^2}{3b^2c^2}| \ll 1$ which ensures a finite overlap in the NLS limit. Here we expand the differential equation (D2) in terms of $1/b$

$$\begin{aligned} L &= b\left(L^{(0)} + b^{-1}L^{(1)} + O(b^{-2})\right) \\ L^\dagger &= b\left(L^{(0)\dagger} + b^{-1}L^{(1)\dagger} + O(b^{-2})\right) \\ \Phi_s &= \Phi_s^{(0)} + b^{-1}\Phi_s^{(1)} + O(b^{-2}) \end{aligned} \tag{D6}$$

At order b^1 eq.(D2) reads

$$\underline{b^1}: \quad L^{(0)\dagger}\Phi_s^{(0)} \ = \ -i\partial_{\zeta\zeta}\Phi_s^{(0)} \ + \ \frac{ic}{b}(2\tanh^2(\kappa\zeta)-1)\Phi_s^{(0)} \ - \ \frac{ic}{b}\tanh^2(\kappa\zeta)\Phi_s^{(0)*} \ = \ 0 \tag{D7}$$

from which one gets $\Phi_s^{(0)} = i/\cosh^2(\kappa\zeta)$. At order b^0 eq.(D2) yields

$$\begin{aligned} \underline{b^0}: \quad L^{(0)\dagger}\Phi_s^{(1)} &= -L^{(1)\dagger}\Phi_s^{(0)} \\ &= i\ \left(\tanh^2(\kappa\zeta)(8-28\kappa^2) + (-4+8\kappa^2)\right)/(3\cosh^2(\kappa\zeta)) \end{aligned} \tag{D8}$$

Using the full fundamental system of $L^{(0)\dagger}$ (irrespective of boundary conditions)

$$\begin{array}{ll} i/\cosh^2(\kappa\zeta) & \dfrac{i}{4\kappa}\cosh(\kappa\zeta)\sinh(\kappa\zeta) + \dfrac{3i}{8\kappa}\tanh(\kappa\zeta) + \dfrac{3i}{8}\dfrac{\zeta}{\cosh^2(\kappa\zeta)} \\ \tanh(\kappa\zeta) & 1-\kappa\zeta\tanh(\kappa\zeta) \end{array} \tag{D9}$$

one can construct the bounded solution

$$\Phi_s^{(1)} = \frac{2-7\kappa^2}{3\kappa^2}\tanh^2(\kappa\zeta) + 1 \tag{D10}$$

Combining $\Phi_s^{(0)}$ and $\Phi_s^{(1)}$ and taking the limit $\zeta \to \infty$ in the terms $O(b^{-1})$ one finds the outer behavior of the inner solution

$$\Phi_s = i/\cosh^2(\kappa\zeta) \ + \ \frac{2-4\kappa^2}{3b\kappa^2} \ + \ O(b^{-2}) \tag{D11}$$

This expression has to be matched to the outer exponential solution. By using eqs.(D3-D5,D11) one finally gets

$$\Phi_s = \frac{i}{\cosh^2(\kappa\zeta)}\left(1+O(b^{-1})\right) \ + \ \frac{2-4\kappa^2}{3b\kappa^2}\ e^{p_3|\zeta|}\left(1 - i\left(\frac{1}{c} + O(b^{-3})\right)\right)(1+O(b^{-1})) \tag{D12}$$

Now we turn to the inhomogeneity of eq.(52). For arbitrary b, c the terms $\Delta\Omega,\ W^{(1)}$ occuring here can be found from the following ansatz describing the standing hole of the perturbed cubic CGLE in the inner region

$$\left(\mu_2\tanh(\mu_1 x) + \mu_3\tanh^3(\mu_1 x)\right)\ \exp\left(i\mu_4\ln\cosh(\mu_1 x) + i\mu_5\tanh^2(\mu_1 x) - i\mu_6 t\right) \qquad \text{with } \mu_i \text{ real} \tag{D13}$$

Taking the NLS limit of the inhomogeneity in eq.(52) and projecting it onto the neutral mode Φ_s then yields the acceleration

$$\frac{\dot v}{v}\left(\frac{3b^4c}{2(b-c)^3}\left(1+O(b^{-1})\right) + \frac{8}{3} - \frac{b}{c} - \frac{2b}{b-c} + O(b^{-1})\right) \ = \frac{16}{15}Re(d) \tag{D14}$$

As stated in Sec.III A the acceleration $\dot v/v$ diverges at the boundary of the core instability (eq.(45)).

[1] see e.g. Y. Kuramoto, *Chemical Oscillations, Waves and Turbulence*, Springer Series in Synergetics Vol. **19**, Springer Verlag (1984); A.C. Newell, in *Propagation in Systems far from Equilibrium*, edited by J.E. Wesfreid, H.R. Brand, P. Manneville, G. Albinet and N. Boccara (Springer, Berlin, 1988) p. 122, and references therein.
[2] S. Popp, O. Stiller, I. Aranson, A. Weber and L. Kramer Phys. Rev. Lett. **70**, 3880, (1993)
[3] W.v. Saarloos, P.C. Hohenberg Physica **D 56**, 303 (1992).
[4] K. Nozaki and N. Bekki, N. Bekki and K. Nozaki, Physics Letters **A 110**, 133 (1985).
[5] O. Stiller, S. Popp and L. Kramer *From the defocusing non-linear Schrödinger to the complex Ginzburg Landau equation*, following paper.
[6] J.S. Langer and V. Ambegaokar, Phys.Rev. **164**, 498 (1967)
[7] H. Sakaguchi, Prog. Theor. Phys. **85**, 417 (1991).
[8] P.Manneville and H. Chaté, Physics Letters **A 171**, 183-188 (1992)
[9] S. Sasa and T. Iwamoto, Physics Letters **A 175**, 289 (1992).
[10] H. Sakaguchi, Prog. Theor. Phys. **84**, 792 (1990).
[11] H. Chaté, Nonlinearity **7**, 185 (1994).
[12] B.I. Shraiman, A. Pumir, W. van Saarloos, P.C. Hohenberg, H. Chaté, M. Holen, Physica **D 57**, 241 (1992).
[13] I.Aranson, L.Kramer and A.Weber, Phys. Rev. Lett. **72**, 2316, (1994)
[14] I.Aranson, L.Kramer and A.Weber, Phys. Rev. E **47**, 3231 (1993)
[15] J.Lega, B.Janiaud, S.Jucquois and V.Croquette, Phys. Rev. A **45**, 5596, (1992); B. Janiaud, S. Jusquois, J. Lega and V. Croquette, in *Pattern Formation in Complex Dissipative Systems*, edited by S. Kai (World Scientific, Singapore, 1992), p 538.
[16] J.-J. Perraud, A. De Wit, E. Dulos, P. Dewel and P. Borckmans, Phys. Rev. Lett. **71** , 1272 (1993).
[17] T.Leweke and M.Provencal, Phys. Rev. Lett. **72**, 3174 (1994)

Figure Captions

Figure 1: Stability diagram for the 1D CGLE. Waves emitted by the standing hole become convectively unstable below the dashed curve EH (Eckhaus instability) and absolutely unstable below the solid curve HS. Outside the region bounded by the solid curve CS the core of the standing hole becomes unstable (Hopf bifurcation for (real) $d < 0$). The CS line is given by eq.(43). Stable standing holes can be found above HS and below CS (upper branch) for $d \leq 0$. The dashed dotted line MO gives the boundary between monotonic (above) and oscillatory (below) interaction for standing holes (see eq.(54)).

Figure 2: Acceleration instability in the perturbed (cubic) CGLE. Comparison of the reduced acceleration $\partial_t v/v$ from theory (full line) and simulations (squares) for $b = 0.5,\ c = 2.0,\ |d| = 0.002$ and varying phase $arg(d)$. The theoretical curve was found from adjusting (numerically) the parameters $\dot{v}$ and $\Delta\Omega$ in eq.(49) leading to $\dot{v}/v = Re(0.6572\, e^{0.6690i}\, d)$, see eq.(53).

Figure 3: Acceleration $\dot{v}$ of a standing hole in the presence of a shock at distance L in the cubic CGLE ($d = 0$). Comparison of simulations (squares) and theory. The parameters r_3, r_4, z in the boundary condition eqs.(54,55) were obtained from the (numerical) nonlinear shock solution (full lines) or from the analytic approximation eq.(56) (dashed lines). (a) monotonic range: $b = 1.0, c = 3.5$; full line: $\dot{v} = 3.395\ e^{-p_4 L}$, dashed line: $\dot{v} = 4.255\ e^{-p_4 L}$ with $p_4 = \kappa - \sqrt{\kappa^2 - 6q^2} \approx 0.4877$ (see eq.(B5)). (b) oscillatory range: $b = 0.5, c = 2.3$; full line: $\dot{v} = 4.361\ e^{-Re(p_3)L}\sin(Im(p_3)L - 1.460)$; dashed line: $\dot{v} = 8.823\ e^{-Re(p_3)L}\sin(Im(p_3)L - 0.874)$; with $p_3 = \kappa + \sqrt{\kappa^2 - 6q^2} \approx 0.8896 + 0.5940i$ (see eq.(B5)).

Figure 4: Snapshot of the modulus $|A| = |A(x)|$ of a stable uniformly moving hole–shock pair in a simulation for $b = 0.5,\ c = 2.3,\ d = +0.0025$. The solution is space periodic with period $P = 48.4$.

Figure 5: Simulations showing the velocity of the hole center $v = v(t)$ of interacting hole–shock pairs (periodic boundary conditions). In Figs.(a),(b),(c) the CGLE parameters were $b = 0.5, c = 2.3, d = +0.0025$ (i.e. far away from the core instability line). (a) relaxation into a constantly moving solution for period $P = 48.4$. (b) selected final state with (almost) harmonic oscillating velocity for period $P = 37.0$. (c) selected final state with anharmonic oscillating velocity for period $P = 40.0$. (d) CGLE parameters $b = 0.21, c = 1.3, d = -0.005$ (near the core instability line); state with oscillating velocity (including change of the direction) for period $P = 50$.

Figure 6: Interacting hole–shock pairs. Velocity $v = v(n, P)$ and bound state distance $L = L(n, P)$ are plotted as function of the period P for different phases $2n\pi$ contained in one period for the CGLE parameters $b = 0.5, c = 2.3, d = -0.0025$. Full lines show stable ($\lambda_{fp} < 0$) and dashed lines unstable ($\lambda_{fp} > 0$) uniformly moving solutions which are predicted (fixed points) by eq.(67). They are compared with (stable) uniformly moving solutions observed in simulations (X). For larger velocities there are more stationary and oscillatory solutions, which have not been included since the analysis is not applicable in that range.

Figure 7: Like Fig.6, but with CGLE parameters $b = 0.5, c = 2.3, d = +0.0025$.

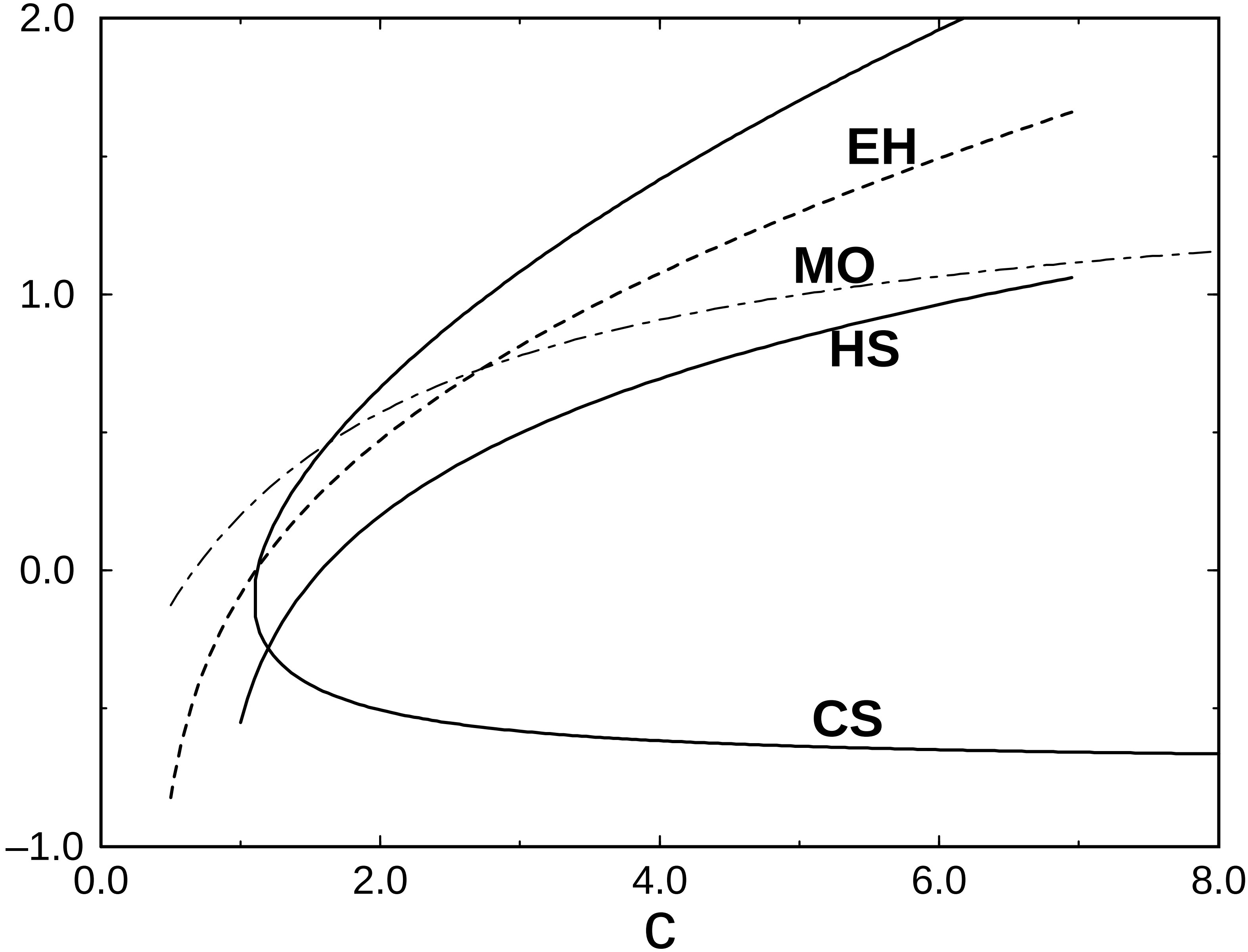

2.0
1.0
0.0
–1.0
0.0
2.0
4.0
6.0
8.0
C
EH
MO
HS
CS

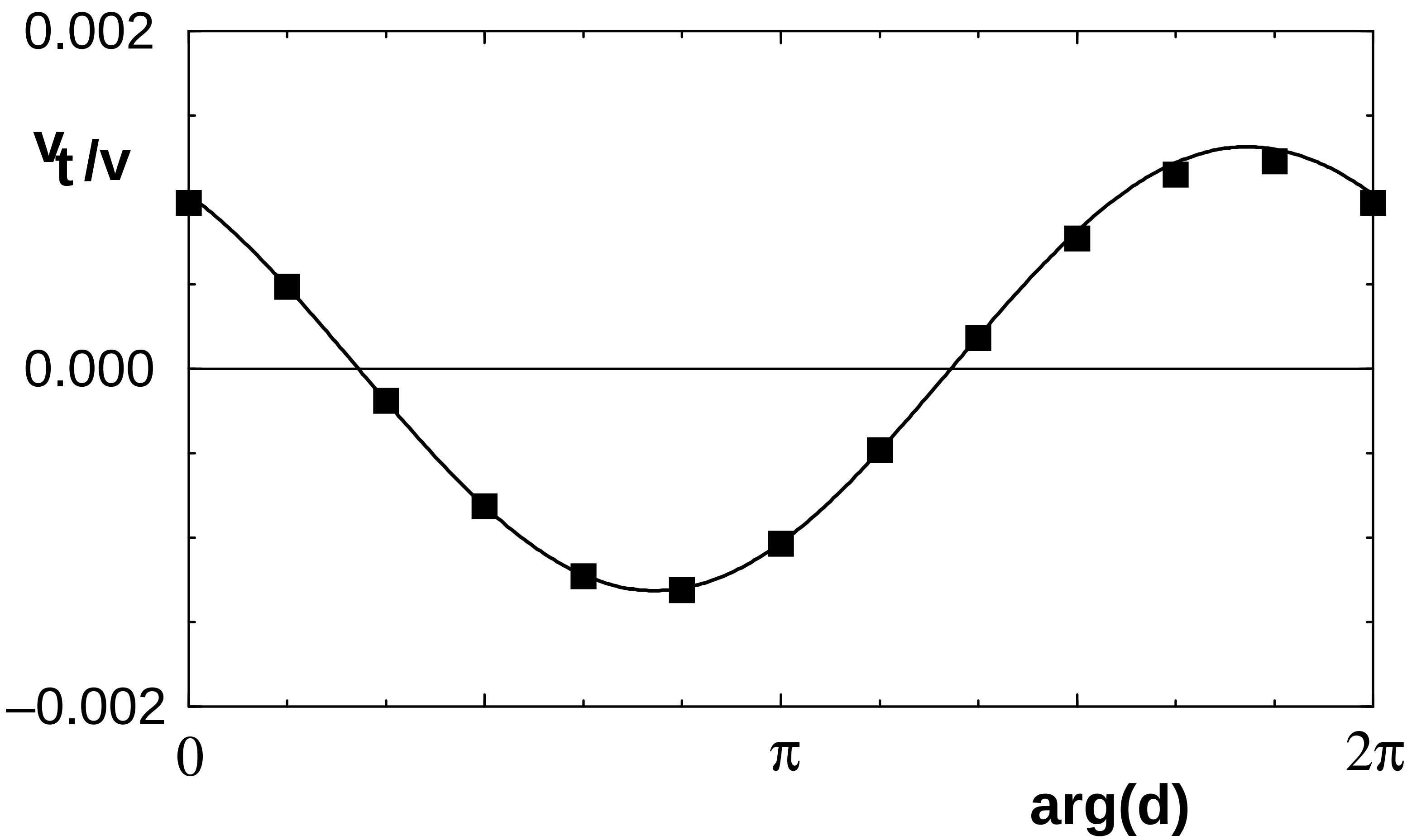

0.002
v_t/v
0.000
–0.002
0
π
2π
arg(d)

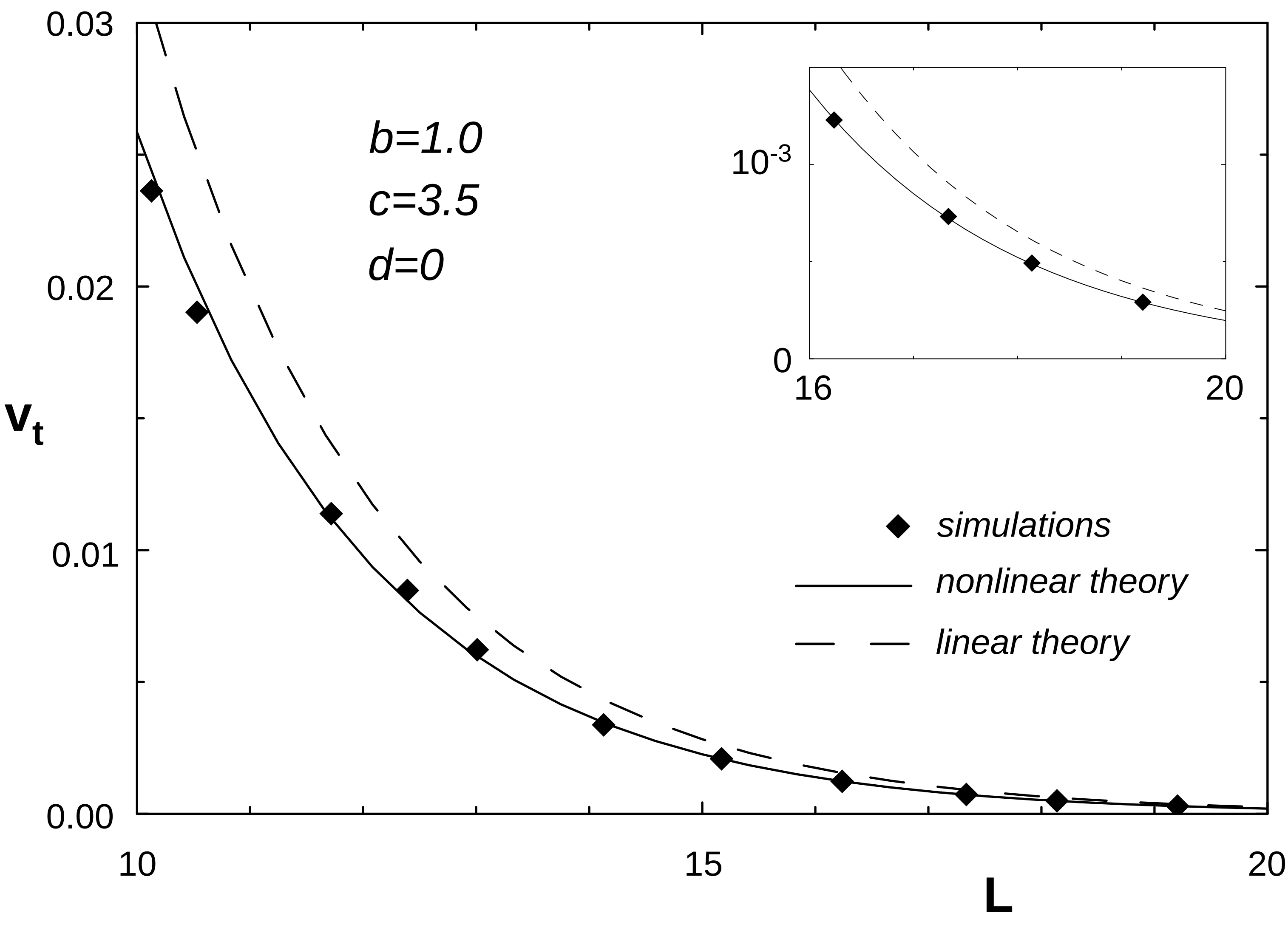

0.03
0.02
0.01
0.00
10
15
20
L
v_t
b=1.0
c=3.5
d=0
10^{-3}
0
16
20
simulations
nonlinear theory
linear theory

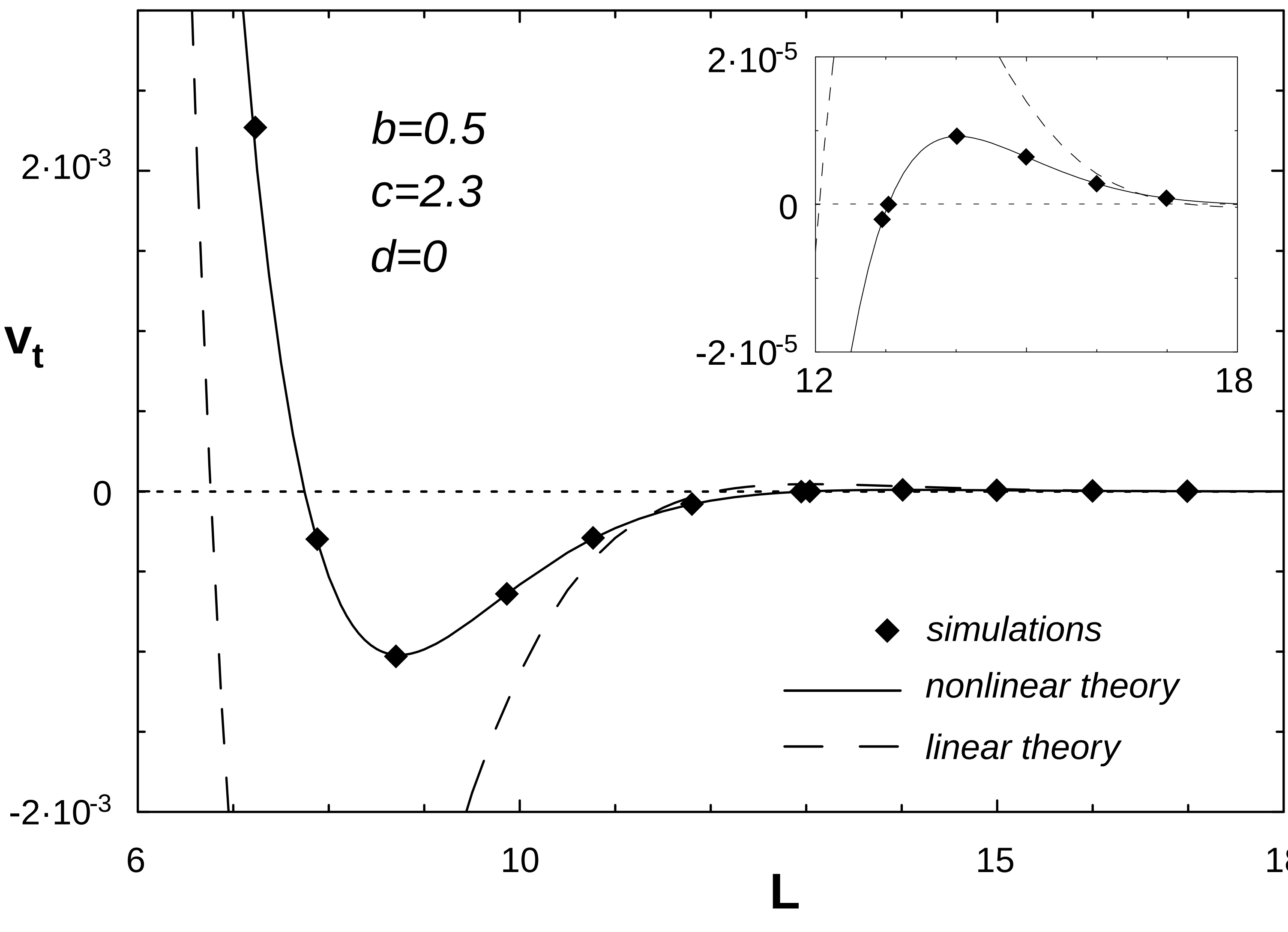

b=0.5
c=2.3
d=0
v_t
$2\cdot10^{-3}$
0
$-2\cdot10^{-3}$
6
10
15
18
L
$2\cdot10^{-5}$
0
$-2\cdot10^{-5}$
12
18
simulations
nonlinear theory
linear theory

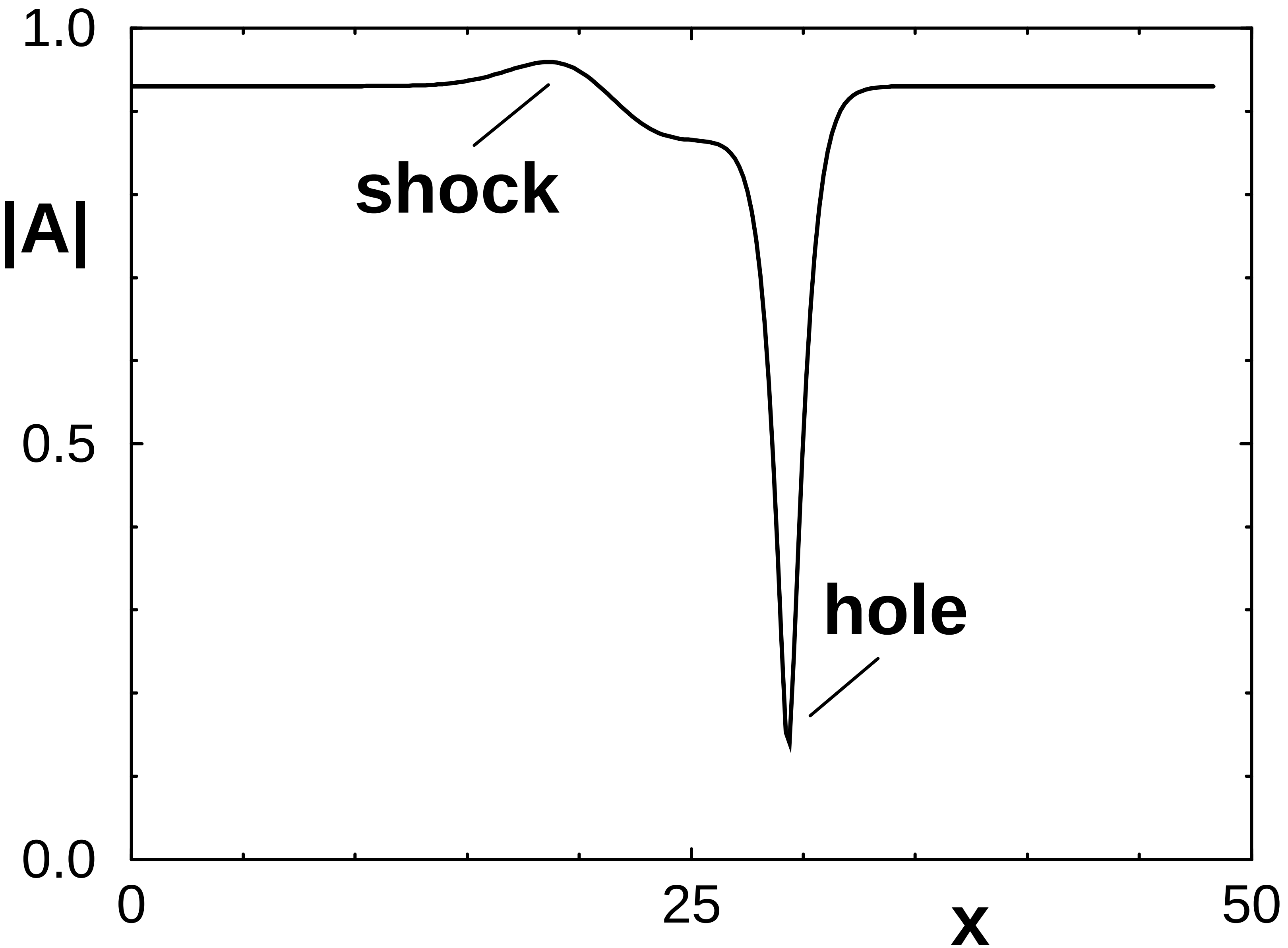

1.0
0.5
0.0
|A|
shock
hole
0
25
50
x

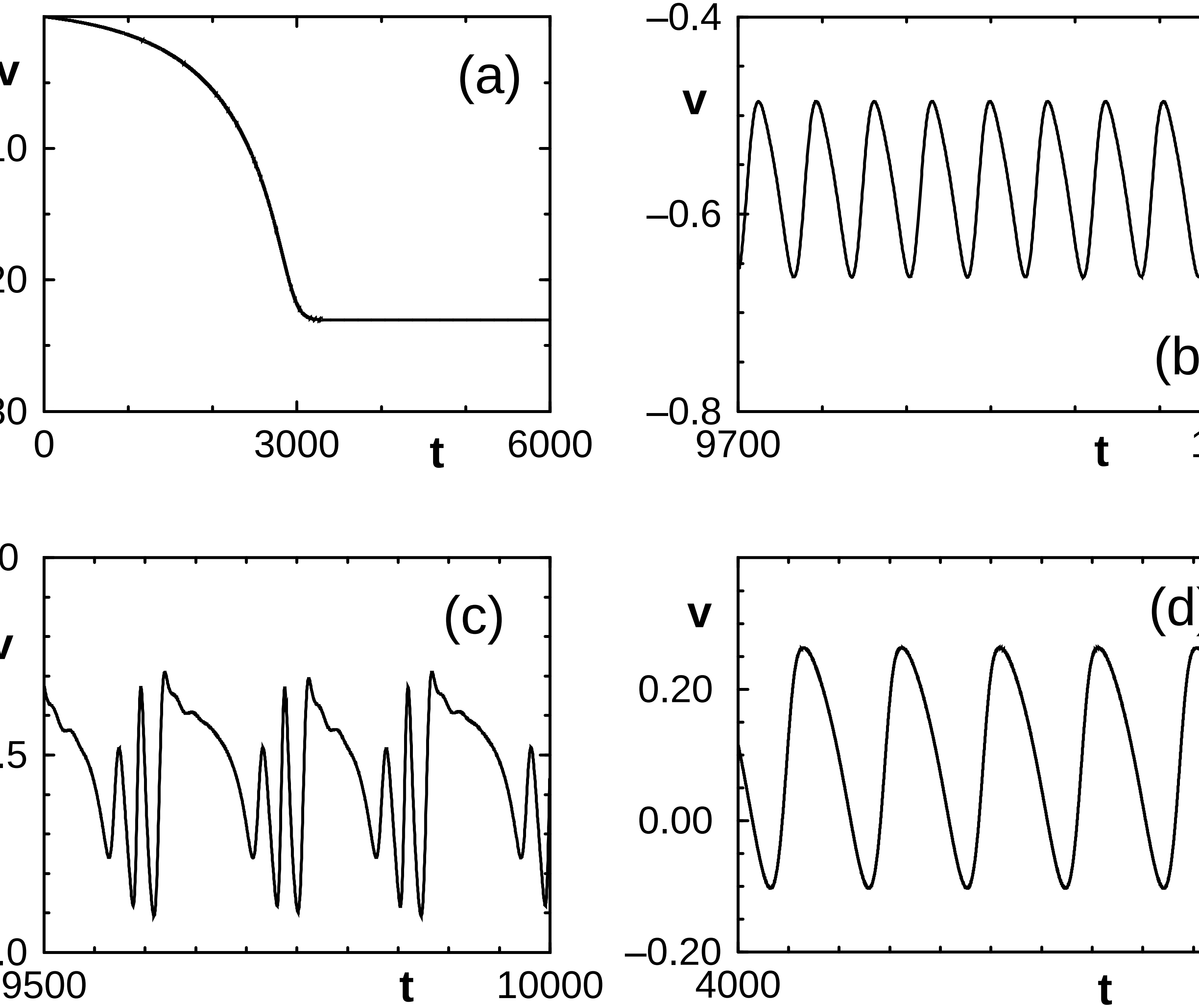
(a)
v
10
20
30
0
3000
6000
t
(b
v
–0.4
–0.6
–0.8
9700
t
(c)
v
0
.5
.0
9500
10000
t
(d)
v
0.20
0.00
–0.20
4000
t

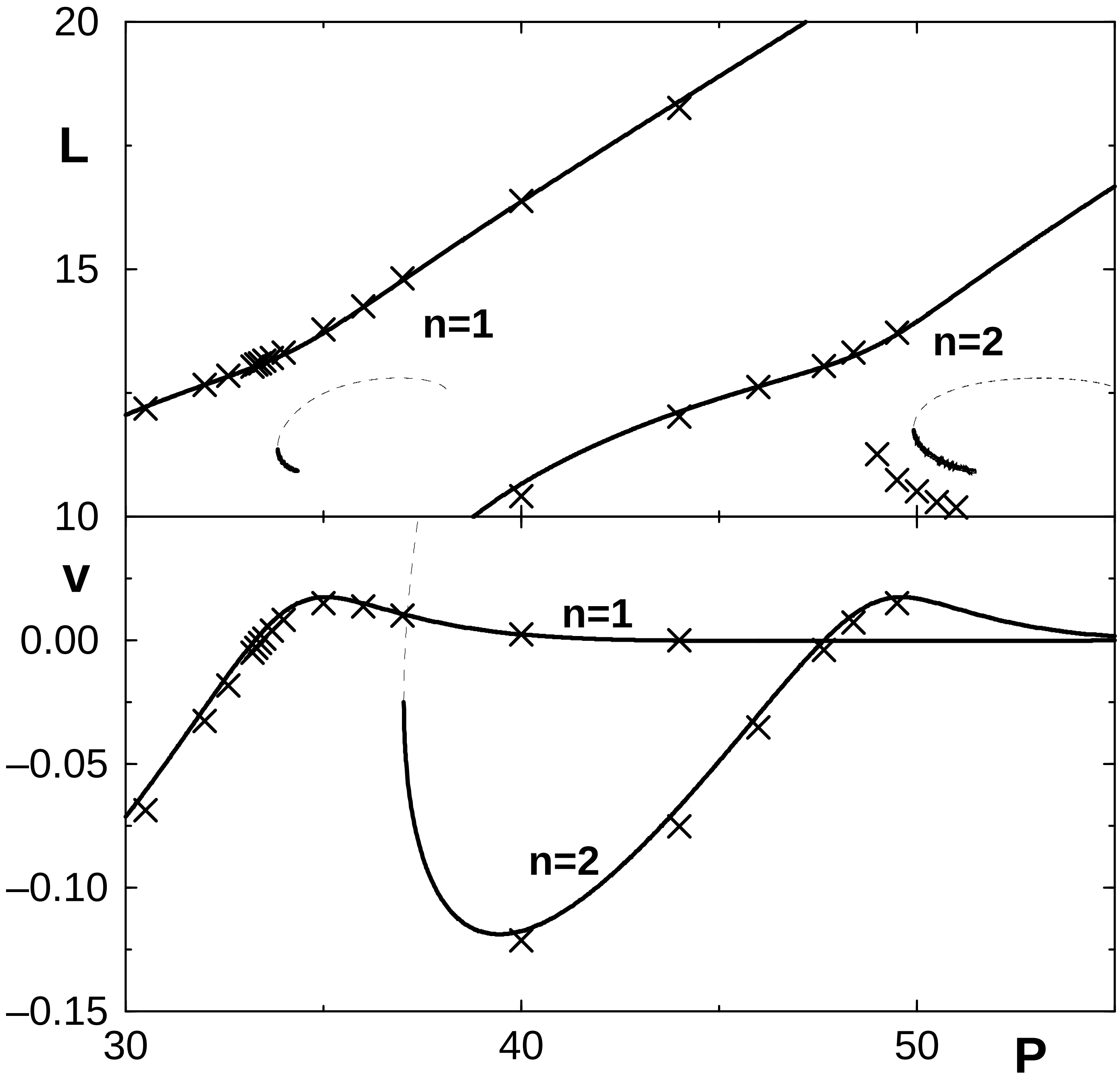
20
L
15
n=1
n=2
10
v
0.00
−0.05
−0.10
−0.15
30
40
50
P

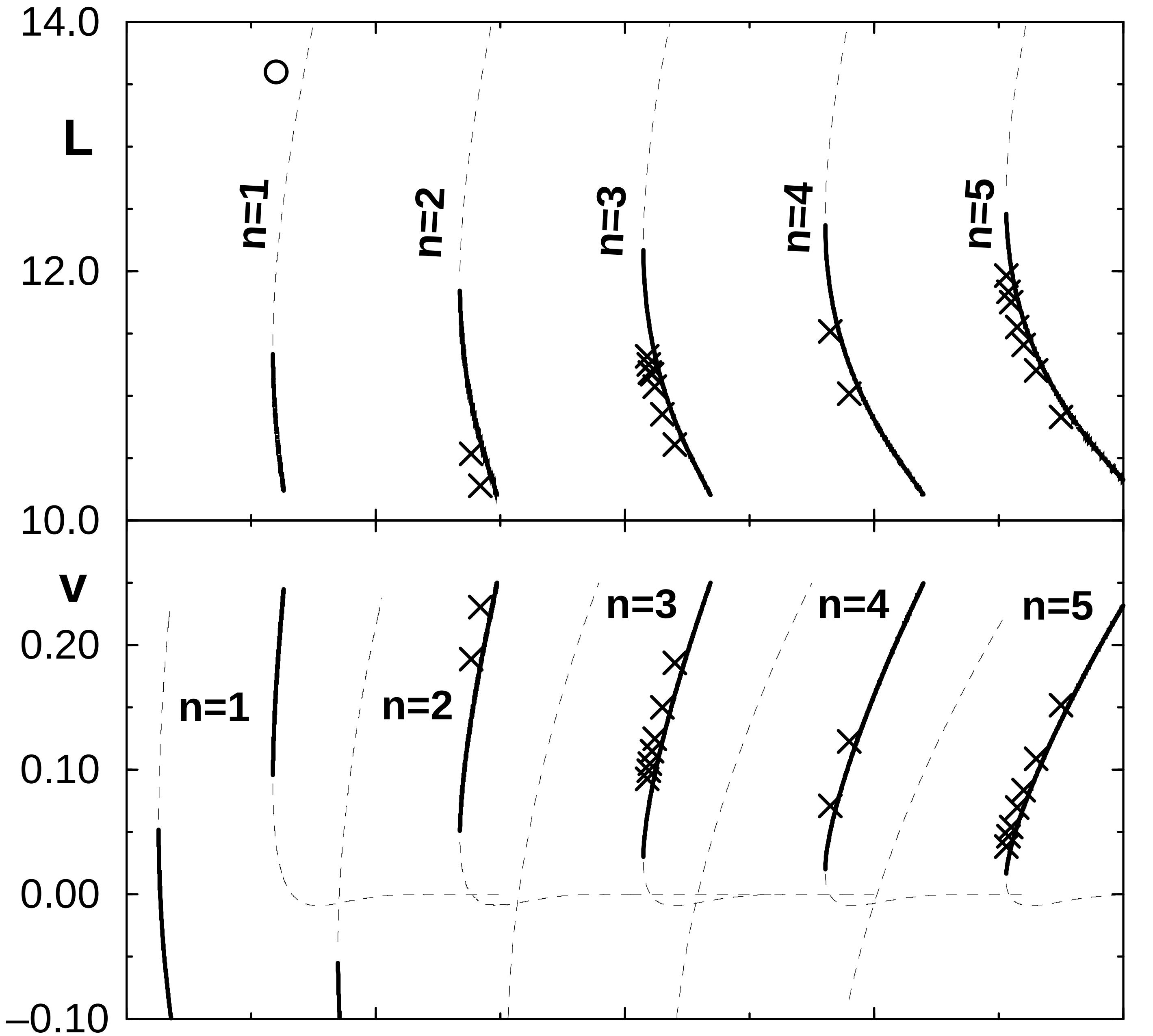
14.0
L
n=1
n=2
n=3
n=4
n=5
12.0
10.0
v
0.20
0.10
0.00
–0.10
20
40
60
80
P
100